Synopsis

of

The Thesis Entitled

"Design, Synthesis and Biological Evaluation of Novel Bruton's Tyrosine Kinase (BTK) Inhibitors"

To be submitted to

The Maharaja Sayajirao University of Baroda

सत्यं शिवं सुन्दरम्

For the Degree

of

DOCTOR OF PHILOSOPHY

In Chemistry

By

Joshi Darshankumar Ashvinbhai

Under the guidance of

Prof. Shubhangi S. Soman

Department of Chemistry,

The Maharaja Sayajirao University of Baroda,

Vadodara-390 002(India)

Dr. Rajesh H. Bahekar

Zydus Research Centre

Zydus Life Sciences Limited

Ahemdabad-382213 (India)

Synopsis of the Thesis

To be submitted to The Maharaja Sayajirao University of Baroda

For the degree of **DOCTOR OF PHILOSOPHY**

Name of the student:	Mr. Joshi Darshankumar Ashavinbhai
Faculty:	Science
Subject:	Chemistry
Name of Guide:	Prof. Shubhangi S Soman (M.Sc. PhD).
Name of Co-Guide:	Dr Rajesh H Bahekar (M. Pharm. PhD).
Title of the Thesis:	"Design, Synthesis and Biological Evaluation of Novel Bruton' Tyrosine Kinase (BTK) Inhibitors"
Registration Number:	FOS/2073
Date of Registration:	27/12/2017
Place of Work:	Department of Medicinal Chemistry, Zydus Research Centre, Ahmedabad Gujarat, India.

Contents of Thesis

Contents

Chapter 1. Introduction and Objective

Introduction

Bruton's tyrosine kinase (BTK) is a cytoplasmic tyrosine kinase of the TEC family. It was named after pediatrician Ogden Bruton, who discovered XLA (X-linked agammaglobulinemia), a disease characterized by the absence of mature B cells. BTK is expressed in the majority of hemopoietic cells, primarily B cells and myeloid cells, but not in T cells or plasma cells. BTK has five domains, such as An N-terminal pleckstrin homology (PH) domain, a Tec homology domain (TH), SRC homology 3 (SH3) and SRC homology 2 (SH2) domains, and a C-terminal kinase domain.

B cell maturation, differentiation, and proliferation were mainly regulated by the B cell receptor (BCR), where the role of the BTK enzyme is very crucial. In the BCR pathway, BTK is activated by the upstream Src-family kinases, such as Blk, Lyn, and Fyn. In turn, BTK phosphorylates and activates phospholipase Cgamma2 (PLCγ2), leading to Ca^{+2} mobilisation and activation of NF-kB and MAP kinase pathways, which are essential for B cell survival. Immune cells like mast cells, basophils, monocytes, and macrophages play important roles in inflammatory and allergic responses. Constitutive BTK activation under autoimmune conditions leads to activation of the Fc receptors of IgG and IgE (FcγR, FcεR), in macrophages and mast cells. BTK is also important for the signalling of chemokine receptors and toll-like receptors (TLRs).

BTK is crucial in the development of inflammatory diseases, mainly autoimmune diseases. Loss of self-tolerance, atypical B cell activation, and the eventual formation of autoreactive antibodies are characteristics of autoimmune diseases. Animal studies demonstrate that BTK is essential for determining the threshold for B cell activation and for the BCR signalling-mediated counter selection of autoreactive B cells. Mutant mice overexpressing BTK rapidly

captured autoimmune disorders like systemic lupus erythematosus (SLE), which affect many organs. BTK is vital for innate immune cells to release inflammatory cytokines. Over activation of BTK could end up resulting in chronic inflammation or an acute hyper inflammatory condition, making BTK inhibition a potential target for treatment for autoimmune disorders.

BTK has been shown to play a key role in several autoimmune disorders like lupus, Rheumatoid arthritis (RA), multiple sclerosis (MS), and various types of B-cell malignancies (mantle cell lymphoma (MCL), chronic lymphocytic lymphoma (CLL), or small lymphocytic lymphoma (SLL)). In the last decade, intense efforts have been made to develop selective BTK inhibitors, especially against closely associated cysteine kinases such as EGFR, JAK3, BLK, BMX, and TEC, for the safe and effective treatment of autoimmune disorders. BTK inhibitors can be classified into two groups based on their chemical scaffold, mode of action, and binding mode. (1) Covalent or irreversible, and (2) non-covalent or reversible.

Ibrutinib (IBR) is the first generation orally administered irreversible BTK inhibitor, which covalently binds to Cys481 of the active adenosine triphosphate (ATP) binding domain of a BTK enzyme. IBR was approved by the FDA in 2013 to treat mantle cell lymphoma (MCL) and was subsequently approved for various indications, such as chronic lymphocytic leukemia (CLL), Waldenström's macroglobulinemia (WM), and marginal zone lymphoma (MZL).

Acalabrutinib and Zanubrutinib are the second-generation irreversible BTK inhibitors that have been approved by the FDA for the treatment of MCL. Other irreversible BTK inhibitors like Tirabrutinib (for BCL), Evobrutinib (for MS), Branebrutinib (for RA, Systemic lupus erythematosus (SLE), and Stevens-Johnson syndrome (SjS)), and Orelabrutinib (for B-cell malignancies and autoimmune diseases) are in clinical development. Reversible BTK inhibitors, Fenebrutinib (for RA and SLE) and Rilzabrutinib (for immune thrombocytopenia (ITP)), are also in clinical development.

Objective

As previously stated, BTK inhibitor is a clinically validated therapeutic target to treat autoimmune diseases, for which a series of BTK inhibitors have been developed, but they have some drawbacks such as off-target activities, poor pharmacokinetic properties, toxicities, etc. Hence, as part of ongoing research, we aim to design and synthesise a safe, potent, and selective BTK inhibitor for the effective treatment of autoimmune disorders like B-cell malignancies and RA.

To achieve these objectives, we worked according to the following steps:

- Design and synthesis of a new series of compounds as BTK inhibitors.
- Characterization of the chemical structures of the synthesised compounds using NMR, UPLC, CHNS, and ESI-MS analysis.
- The *in vitro* activities of all synthesised compounds evaluated using the BTK enzyme inhibition assay and the TMD8 cell proliferation assay.
- *In vitro* active compounds evaluated for CYP and hERG inhibitory activities.
- *In vivo* pharmacokinetic studies of compounds that are devoid of CYP and hERG will be assessed.
- *In vivo* Pharmacological screening studies of the lead compounds
- Evaluation of anti-tumor activity using the TMD8 xenograft model
- Evaluation of the anti-arthritic efficacy using the collagen-induced arthritis (CIA) mice model
- Evaluation of the safety profile
- Evaluation of Kinase selectivity and Irreversible binding to the BTK enzyme of the lead compounds
- Molecular modelling studies of lead compounds

Chapter 2. Results and Discussion

2.1. Design strategy

As described in the BTK inhibitors section, most of the advanced BTK inhibitors are covalent. Covalent inhibition of kinases by targeting a non-catalytic cysteine residue is a validated strategy for achieving sustained target engagement without requiring high systemic drug exposure. In the BTK enzyme structure, Cys481 is proximal to the ATP binding site, and that analogous cysteine residue is present in a few other human kinases. The relatively low prevalence of the corresponding cysteine residue in the human kinome makes covalent inhibition of BTK an attractive strategy for achieving high selectivity.

Based on the co-crystal structure of IBR with BTK enzyme, IBR structure can be categorized into four parts: Hinge binder, Amine linker, Aromatic backbone, and Warhead. The hinge binder (pyrazolo [3,4-d]pyrimidin-4-amine) forms hydrogen bonding with the Met477 (at hinge region) and Glu475, in the active site of BTK. These interactions are very crucial for the BTK inhibitory activity. While piperidine amine acts as a linker and provides spatial angle so that warhead (acrylamide moiety) can interact covalently with Cys481.

Aromatic backbone (biphenyl ether) orients towards the back side pocket of Thr474 and exhibit π-π stacking interactions with the Phe540 of a BTK enzyme. The crucial hinge binder pyrazolo[3,4-d]pyrimidin-4-amine core was considered as a starting point. In the present investigation, stepwise structural modifications were carried out in the IBR to discover novel, potent, selective and orally bioavailable BTK inhibitor. Initially, to improve BTK enzyme selectivity, while retaining potency, a series of compounds (**24a-h**) were designed to identify the novel amine linker. Subsequently, to optimise the aromatic backbone, warhead moiety, and

central core, the second (**32a-an**), third (**32ao-av**), and fourth (**41**, **42**, **51**, **52**, **61**, **62**, **71**, and **72**) series of compounds were designed.

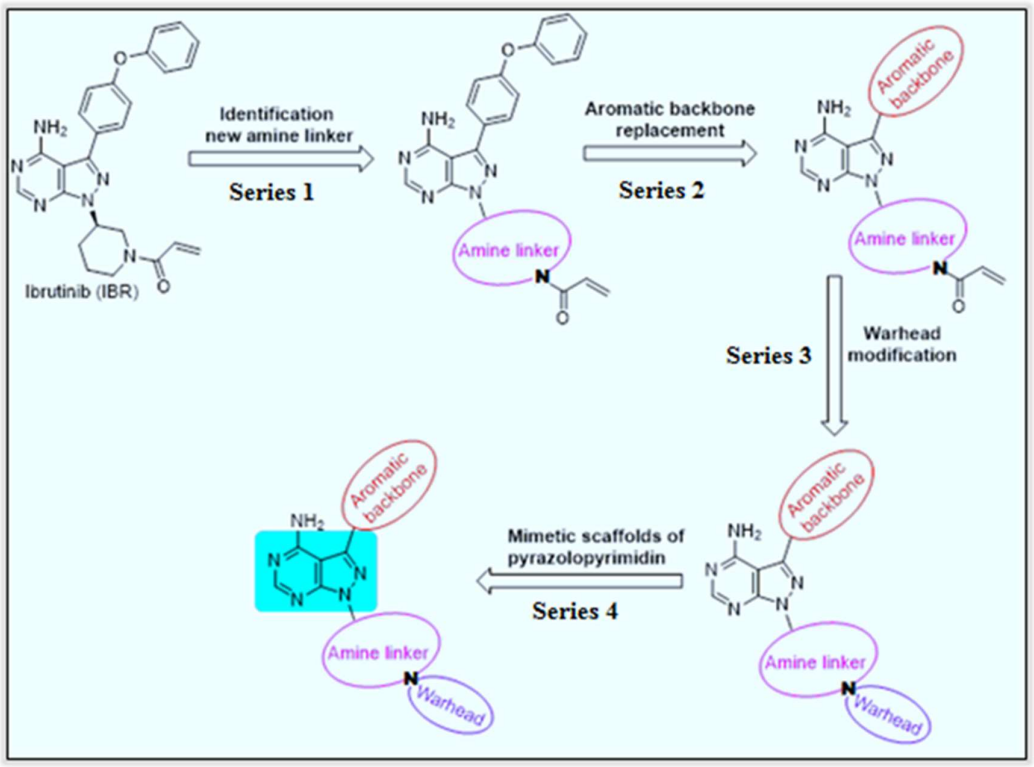

The amine linker is an integral part of BTK inhibitors that provide spatial orientation to the warhead. As per the findings, the piperidine or pyrrolidine ring functions as amine linkers in most of the known BTK inhibitors. According to preliminary molecular modelling results, there is enough space in the ATP binding site of BTK to accommodate a saturated bicyclic ring system. Hence, in **Series 1**, we have selected some saturated bicyclic amines as linkers for bioisosteric replacement of piperidine in IBR and synthesised a total of eight target compounds (**24a-h**) by employing **Scheme 4**.

After discovering the amine linker, which has superior biological potency in **Series 1**, we will make subsequent efforts to optimise the aromatic backbone component of the BTK inhibitor in **Series 2**. According to a molecular modelling analysis, the aromatic backbone adopts a favourable orientation in the hydrophobic pocket of the BTK enzyme, enabling it to interact with the vital residues (Thr474 and Phe540) of the hydrophobic pocket. The docking study

additionally revealed that if a hydrogen bond acceptor is introduced into the aromatic backbone, additional hydrogen bond interactions with Ser538 and/or Lys430 may occur, eventually leading to kinase selectivity.

These findings led to the selection of three sets of aromatic backbone bioisosteres in **Series 2**. In the first set of **Series 2**, benzamide and picolinamide derivatives were designed, whereas in the second set of **Series 2**, 4-phenyl ether, 4-phenyl thioether, and 4-phenyl alkyl derivatives were used as the aromatic backbones. Phenyl-containing fused heterocycles were enlisted as the aromatic backbone for the third set of **Series 2**. In accordance with the synthetic route given in **Scheme 6**, forty compounds (**32a-an**) prepared in **Series 2** and screened for *in vitro* activities.

Electrophilic warheads, which feature in the design of BTK inhibitors, interact covalently with the nucleophilic Cys481 of the BTK enzyme. In **Series 3**, to study the influence of warheads on BTK inhibitory activities, selected Michael acceptors and other moiety were utilised as warheads instead of conventional acrylamide. In **Series 3**, a total of eight compounds (**32ao-av**) were synthesised using **Scheme 7**,

Pyrozolo-pyrimidine-4-amine is a key pharmacophore and interacts with the hinge region of BTK enzyme through the hydrogen bonding. It also provides orientation to the aromatic backbone and linker, which create a "Y" shape that is essential for BTK inhibitory activities. In **Series 4**, we intended to incorporate certain mimetic heterocycles of Pyrazolo-pyrimidine, such as Pyrrolo-pyrimidin, Oxo-purine, Imidazo-pyrazine, and Pyrazole scaffolds, in place of Pyrazolo-pyrimidine. In **Series 4**, eight compounds (**41**, **42**, **51**, **52**, **61**, **62**, **71**, and **72**) were synthesised following the synthetic method described in **Schemes 8**, **9**, **10**, and **11**.

2.2. 3-(4-phenoxyphenyl)-pyrazolo[3,4-d]pyrimidin-4-amine scaffold based BTK inhibitors 24a-h (Series 1)

In our initial investigation, we selected eight saturated bicyclic amine rings for bioisosteric replacement of piperidine in IBR and synthesised eight target compounds (**24a-h**) in the **Series 1** as novel BTK inhibitors.

The synthesised compounds (**24a–h**) were assessed for their *in vitro* BTK inhibitory activity using a cell-free biochemical assay. Briefly, a fixed amount of recombinant purified human BTK (3 ng/reaction) was incubated with increasing concentrations of test compounds. An enzymatic reaction was initiated by adding a substrate cocktail containing ATP (50 μmol/L) to 96-well plates. The reaction was incubated at room temperature for 2 h, followed by quantification of the leftover ATP, according to the manufacturer's protocol, using ADP-Glo reagent. Data were plotted using 'enzyme with no inhibitor' as the 100% kinase

The anti-proliferative activity of test compounds (**24a-h**) were evaluated *in vitro* in the human diffuse large B-cell lymphoma (DLBCL) cell line TMD8. Briefly, defined numbers of TMD8 cells were incubated in 96-well plates with increasing concentrations of test compounds. Cell growth was measured using the MTT assay, and IC_{50} values were determined by nonlinear regression using the Graph Pad Prism 6 software. IBR was taken as the positive control, and it showed IC_{50} values of 1.1 nM and 1.2 nM in the BTK enzyme and TMD8 cell proliferation assays, respectively.

Scheme 1: Synthetic route of 24a-h of Series 1

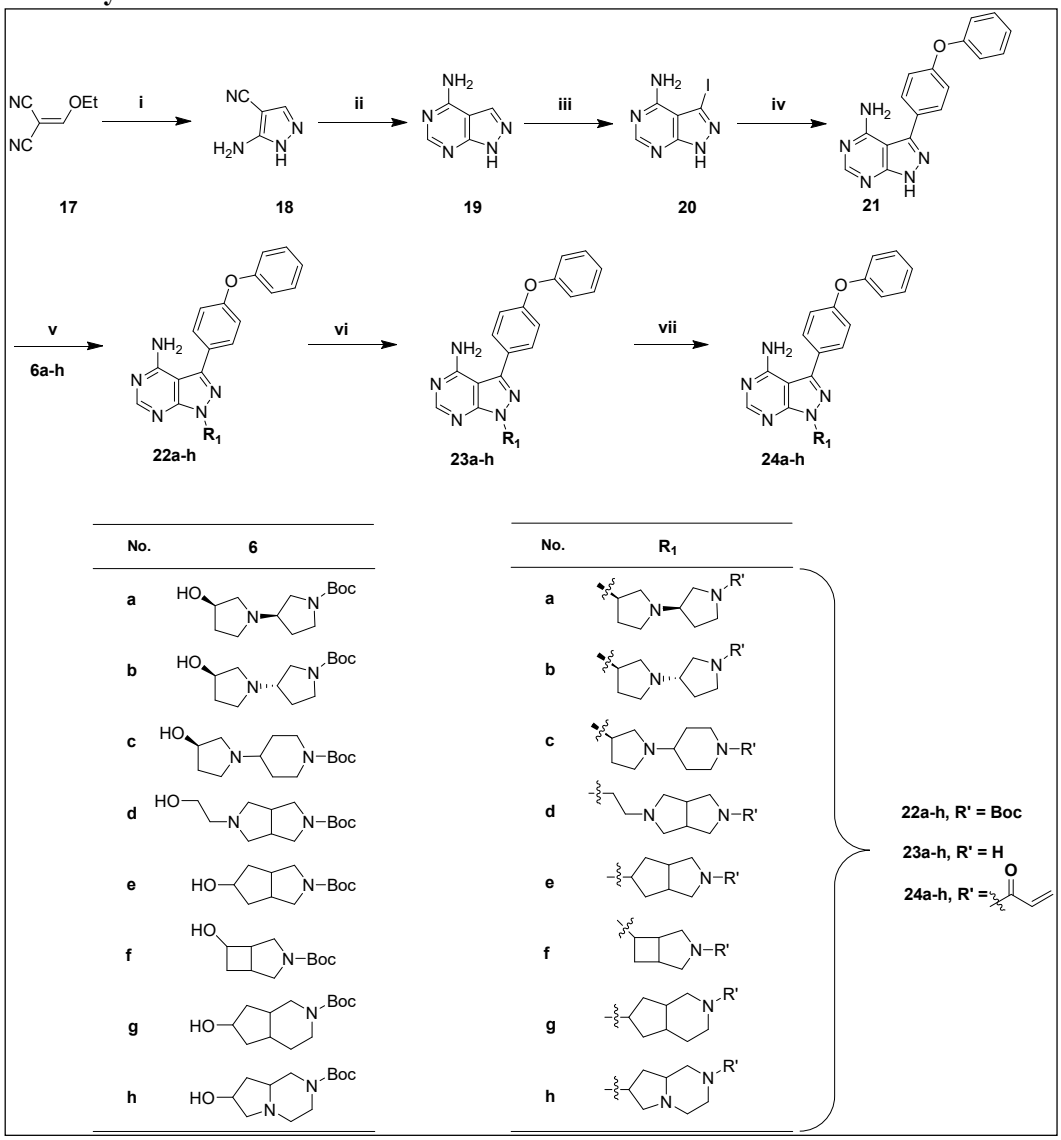

Reagents and conditions: i) Hydrazine hydrate, 110ºC, 3 h, 69%; ii) Formamide, 180ºC, 5 h, 87%; iii) N-iodosuccinimide, DMF, 80ºC, 18 h, 85%; iv) 4-phenoxyphenyl boronic acid, $PdCl_2(PPh_3)_2$, $KHCO_3$(aq), DMF, 90ºC, 5 h, 74%; v) **6a-h**, diisopropyl azodicarboxylate, triphenyl phosphine, THF, 25°C, 18 h, 43-68%; vi) Trifluoroacetic acid, DCM, 25°C, 3 h, 87-95%; vii) Acryloyl chloride, N,N-Diisopropylethylamine, DCM, 0°C to 25°C, 18 h, 38-63%.

Biological evaluation of Series 1

Table 1. *In vitro* BTK enzyme and TMD8 cell proliferation inhibitory data of 24a–h of Series 1

Comp.	R_1	BTK IC_{50} (nM)[a]	TMD8 IC_{50} (nM)[b]	Comp.	R_1	BTK IC_{50} (nM)[a]	TMD8 IC_{50} (nM)[b]
24a		5.1	4.4	**24e**		1.4	0.5
24b		2.8	1.4	**24f**		29	21
24c		38	46	**24g**		2.9	2.8
24d		8.1	11	**24h**		3.6	3.3
	IBR	1.1	1.2				

Table 2. CYP and hERG inhibitory activity of the lead compound of Series 1

Comp.	%hERG inhibition[a] @ 10 µM	% CYP inhibition[b]@ 10 µM					
		CYP1A2	CYP2C8	CYP2C9	CYP2D6	CYP2C19	CYP3A4
24e	54	14	16	40	19	9	8
IBR	35	NI	**81**	**86**	31	39	**55**

Table 3. Pharmacokinetic profile[a] of 24e

Dose	Parameters	24e		IBR	
		Mice	*Rat*	*Mice*	*Rat*
IV 1 mg kg^{-1}	AUC (ng.h/mL)	401	370	151	250
	Vss (L/kg)	0.90	1.37	0.50	1.50
	CL (ml/min/kg)	48.1	49.9	27.5	66.3
	$T_{1/2}$ (h)	0.35	0.39	0.20	0.40
PO 3 mg kg^{-1}	T_{max} (h)	0.25	0.25	0.25	0.25
	C_{max} (ng/mL)	282	283	402	129
	AUC (ng.h/mL)	433	301	277	86
	$T_{1/2}$ (h)	0.56	1.08	0.30	0.80
	%F*	**36**	**25**	**15**	**11**

Molecular docking study of 24e of Series 1

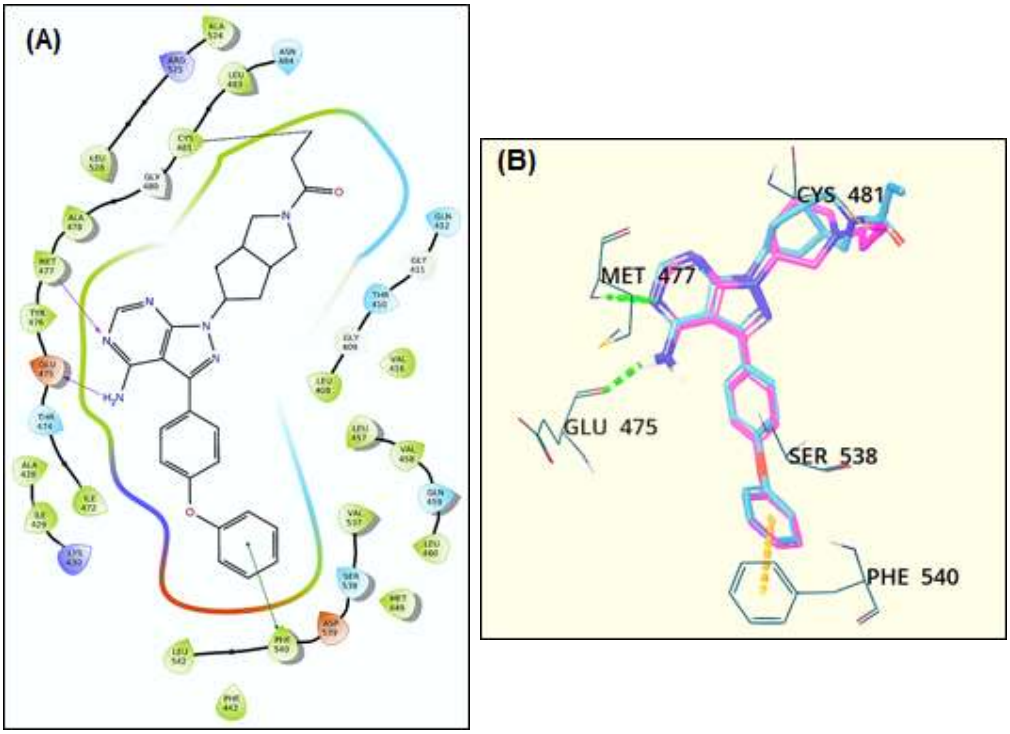

Figure represents the resemblance of the binding poses of **24e** (azure) and IBR (salmon pink) in the active site of BTK enzyme. At the hinge region of the BTK domain, the amino group of the pyrimidine ring of **24e** forms an H-bond with the backbone carbonyl of Glu474, while the pyrimidine ring nitrogen forms an H-bond with the backbone NH of Met477. Both IBR and **24e** evidenced important interactions with the thiol group of Cys481 of BTK, which binds covalently as Michael adducts. Through "T" shape π-π stacking, the phenoxy phenyl ring interacts with Phe540. Overall, **24e** and IBR bind to the active domain of the BTK enzyme with the same alignment, confirming its in vitro BTK inhibitory activity. Additional interactions of **24e** with Gln412 in the catalytic domain of the BTK enzyme are likely to contribute to BTK inhibitory activity. IBR and **24e** docking scores were found to be -11.08 and -11.15 kcal mol-1, respectively.

2.3. 1-(octahydrocyclopenta[c]pyrrol-5-yl)-1H-pyrazolo[3,4-d]pyrimidin-4-amine scaffold based BTK inhibitors 32a-an (Series 2)

In preliminary research from **Series 1**, we discovered the octahydrocyclopenta[c]pyrrole analogue (**24e**) to be a superior bioisosteric alternative to piperidine, and its biological potency motivated us to make subsequent efforts to optimise the aromatic backbone component of the BTK inhibitor **24e** (**Figure 14**).

For optimisation and bioisosteric replacement of phenoxy phenyl, three sets of aromatic backbones were selected in **Series 2**. In the first set of **Series 2**, benzamide (**32a-e, 32j-k**) and picolinamide (**32f-i**) derivatives were designed, whereas in the second set of **Series 2**, 4-phenyl ether (**32l-q**), 4-phenyl thioether (**32r-v**), and 4-phenyl alkyl (**32w-aa**) derivatives were used as the aromatic backbones. Phenyl-containing fused heterocycles (**32ab-an**) were enlisted as the aromatic backbone for the third set of **Series 2**. In total, forty compounds (**32a–an**) were synthesized in the **Series 2**, and their *in vitro* activities were evaluated.

Scheme 2: Synthetic route of 32a-an of Series 2

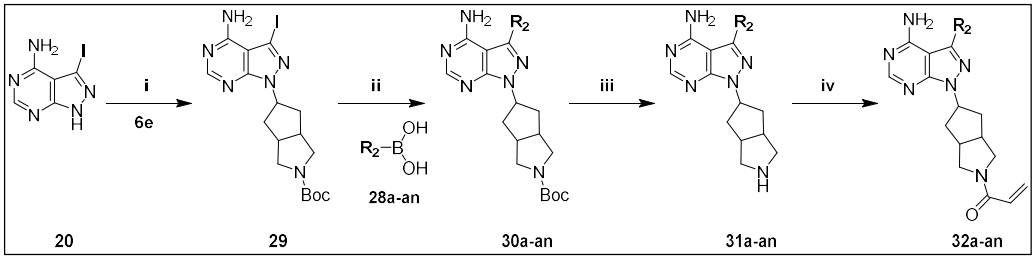

Reagents and conditions: i) diisopropyl azodicarboxylate, triphenyl phosphine, THF, 25°C, 18 h, 66%; ii) R_2-boronic acid (**28a-an**), $PdCl_2(PPh_3)_2$, $KHCO_{3(aq)}$, DMF, 90ºC, 5 h, 42-76%; iii) Trifluoroacetic acid,, DCM, 0°C to 25°C, 3 h, 73-92%; iv) Acryloyl chloride, N,N-Diisopropylethylamine, DCM, 0°C to 25°C,18 h, 35-68%.

Set 1: benzamide and picolinamide-based derivatives (**R_2**)

No.	R_2
a	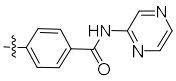
b	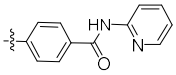
c	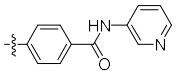
d	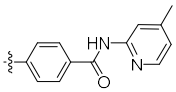
e	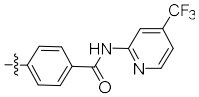
f	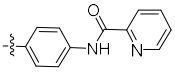
g	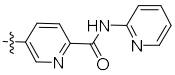
h	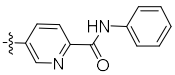
i	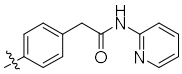
j	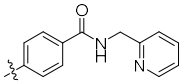
k	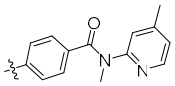

Set 2: 4-phenyl ether, 4-phenyl thioether, and 4-phenyl alkyl-based derivatives (**R_2**)

No.	R_2
l	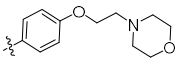
m	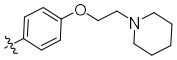
n	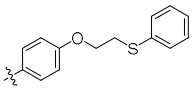
o	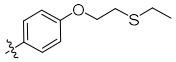
p	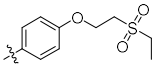
q	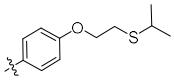
r	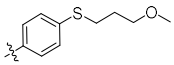
s	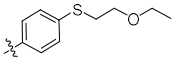
t	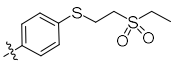
u	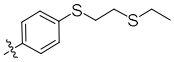
v	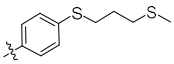
w	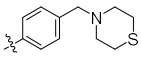
x	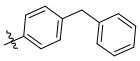
y	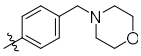
z	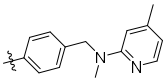
aa	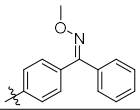

Set 3: Phenyl-containing fused heterocycle-based derivatives (**R_2**)

No.	R_2
ab	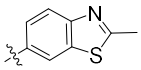
ac	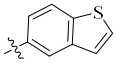
ad	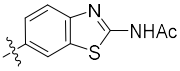
ae	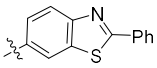
af	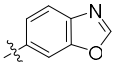
ag	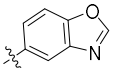
ah	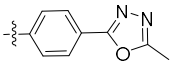
ai	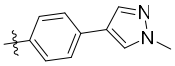
aj	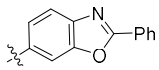
ak	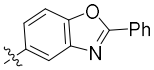
al	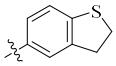
am	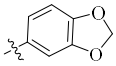
an	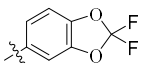

Biological evaluation of Series 2

Table 4. ***In vitro*** **BTK enzyme and TMD8 cell proliferation inhibitory data of 32a-an of Series 2**

Comp.	R_2	BTK IC_{50} (nM)[a]	TMD8 IC_{50} (nM)[b]	Comp.	R_2	BTK IC_{50} (nM)[a]	TMD8 IC_{50} (nM)[b]
32a	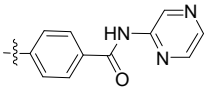	4.4	4.3	**32u**	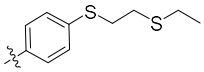	0.8	0.4
32b	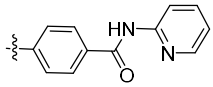	1.0	0.8	**32v**	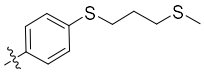	0.8	1.7
32c	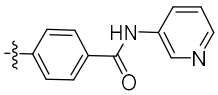	4.0	3.9	**32w**	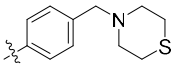	>100	>100
32d	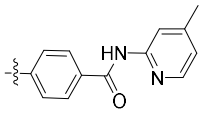	0.6	0.4	**32x**	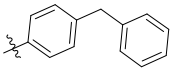	6.0	2.3
32e	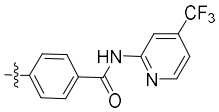	0.6	0.2	**32y**	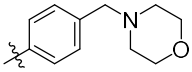	>100	>100
32f	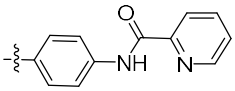	8.1	7.2	**32z**	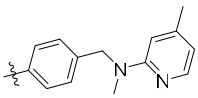	62.5	82.4
32g	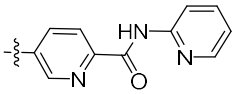	7.5	7.1	**32aa**	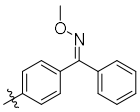	10.5	10.9
32h	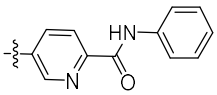	7.6	7.8	**32ab**	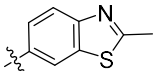	>100	>100
32i	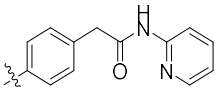	68.5	79.2	**32ac**	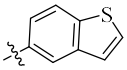	6.6	6.8
32j	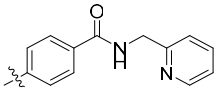	55.4	71.3	**32ad**	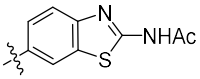	41.3	59.5
32k	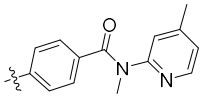	25.7	33.2	**32ae**	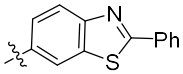	18	26.9
32l	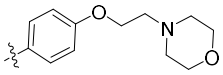	>100	>100	**32af**	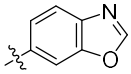	>100	>100
32m	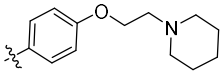	>100	>100	**32ag**	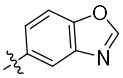	38	46.2
32n	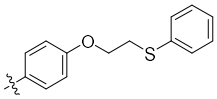	11.7	12.7	**32ah**	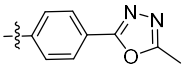	5.6	7.1
32o	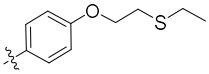	8.3	8.8	**32ai**	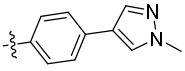	>100	>100
32p	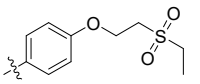	89	82	**32aj**	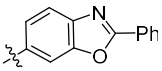	>100	>100

32q	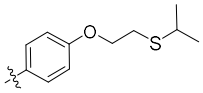	14.6	7.5	**32ak**	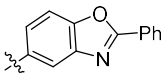	5.6	8.7
32r	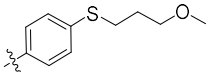	10.4	10.8	**32al**	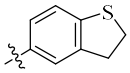	4.0	3.5
32s	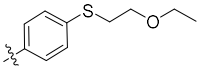	9.4	8.5	**32am**	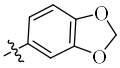	11.7	9.3
32t	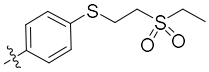	18.9	13.7	**32an**	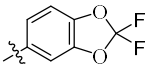	51.1	>100
	IBR	1.1	1.2				

Table 5. CYP and hERG inhibitory activity of the lead compounds of Series 2

Comp.	%hERG[a] inhibition @ 10 µM	% CYP inhibition[b] @ 10 µM					
		CYP1A2	CYP2C8	CYP2C9	CYP2D6	CYP2C19	CYP3A4
32b	NI	NI	12	19	17	1	12
32d	26	13	27	**63**	34	27	2
32e	**63**	NI	**63**	**79**	27	38	33
32u	32	18	**75**	**79**	**60**	**63**	**63**
32v	44	12	**72**	**58**	**69**	50	40
IBR	35	NI	**81**	**86**	31	39	**55**

Table 6. Pharmacokinetic profile[a] of 32b

Dose	Parameters	32b		IBR	
		Mice	*Rat*	*Mice*	*Rat*
IV 1 mg kg $^{-1}$	AUC (ng.h/mL)	422	479	151	250
	Vss (L/kg)	0.70	0.88	0.50	1.50
	CL (ml/min/kg)	39.5	36.0	27.5	66.3
	$T_{1/2}$ (h)	0.40	0.60	0.20	0.40
PO 3 mg kg $^{-1}$	T_{max} (h)	0.25	0.25	0.25	0.25
	C_{max} (ng/mL)	703	794	402	129
	AUC (ng.h/mL)	588	1074	277	86
	$T_{1/2}$ (h)	0.80	2.00	0.30	0.80
	%F*	**47**	**75**	**15**	**11**

Molecular docking study of 32b of Series 2

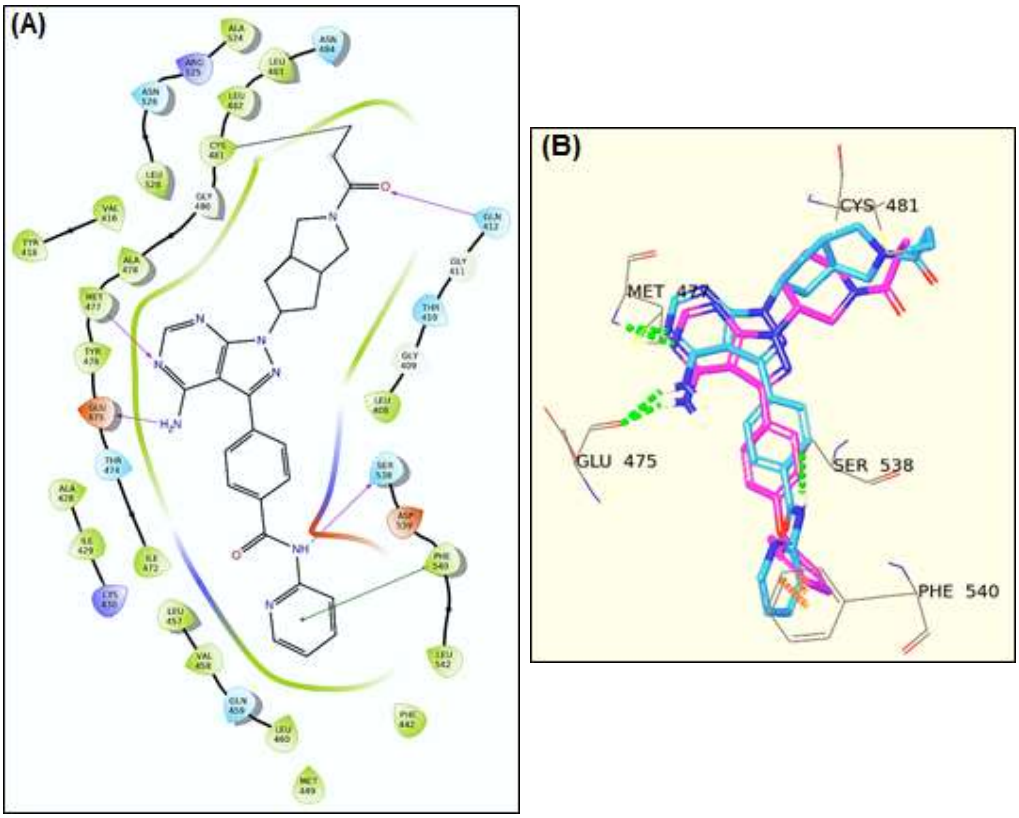

The binding orientations of **32b** (azure) and IBR (salmon pink) in the active site of the BTK enzyme are the same, as shown in **Figure 15**. The pyrimidine ring nitrogen forms an H-bond with the backbone NH of Met477 in the hinge region of the BTK domain, while the amino group of the pyrimidine ring **32b** forms an H-bond with the backbone carbonyl of Glu474. With the thiol group of Cys481 in BTK, which binds covalently as Michael adducts, both IBR and **32b** revealed significant interactions. Through "T" shape π-π stacking, the N-2-pyridyl ring interacts with Phe540. Eventually, **32b** and IBR have the same alignment when they bind to the active domain of the BTK enzyme, establishing their *in vitro* BTK inhibitory activity. An additional bonding of **32b** in the catalytic domain of BTK enzyme with Ser538 and Gln412 is believed to be contributing to its potent BTK inhibitory activity. The docking scores of IBR and **32b** were -11.08 and -11.89 kcal/mol, respectively.

2.4. 4-(4-amino-1-(octahydrocyclopenta[c]pyrrol-5-yl)-1H-pyrazolo[3,4-d]pyrimidin-3-yl)-N-(pyridin-2-yl)benzamide scaffold based BTK inhibitors 32ao-av (Series 3)

The nucleophilic Cys481 of the BTK enzyme interacts covalently with electrophilic warheads, which is an essential component of BTK inhibitor structures. **32b** of **Series 2** was found to be highly potent (BTK enzyme and TMD8 cell proliferation assays, IC_{50} values of 1.0 and 0.8 nM, respectively) and devoid of hERG and CYP liabilities (<50% inhibition at 10 µM concentration) when using a conventional acrylamide warhead. To study the influence of warheads on *in vitro* activity, selected Michael acceptors and other moiety (R_3) were used as warheads instead of acrylamide, and eight compounds **32ao-av** were synthesized in **Series 3**

Scheme 3: Synthetic route of 32ao-av of Series 3

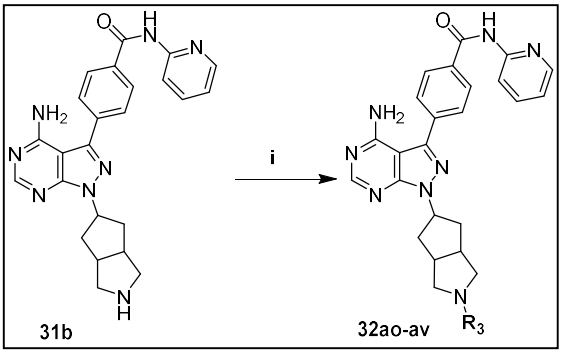

No.	R_3	No.	R_3	No.	R_3
ao	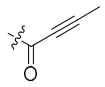	ar	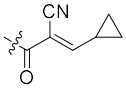	au	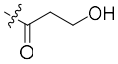
ap		as		av	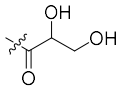
aq	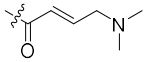	at			

Reagents and conditions: i) R_3-Acid, O-(1H-Benzotriazol-1-yl)-N,N,N',N'-tetramethyluronium hexafluorophosphate, N,N-Diisopropylethylamine, DMF, 0°C to 25°C,18 h, 42-71%;

Biological evaluation of Series 3

Table 7. *In vitro* BTK enzyme and TMD8 cell proliferation inhibitory data of 32ao-av of Series 3

Comp.	R_3	BTK IC_{50} (nM)[a]	TMD8 IC_{50} (nM)[b]
32ao		1.2	0.9
32ap		4.9	3.9
32aq		5.2	4.7
32ar		>100	83
32as		6.2	5.8
32at		48.2	61.4
32au		>100	>100
32av		>100	>100
	IBR	1.1	1.2

Table 8. CYP and hERG inhibitory activity of the lead compound of Series 3

Comp.	%hERG[a] inhibition @ 10 µM	% CYP inhibition[b] @ 10 µM					
		CYP1A2	CYP2C8	CYP2C9	CYP2D6	CYP2C19	CYP3A4
32ao	23	NI	NI	28	15	18	16
IBR	35	NI	**81**	**86**	31	39	**55**

Table 9. Pharmacokinetic profile[a] of 32ao

Dose	Parameters	32ao		IBR	
		Mice	*Rat*	*Mice*	*Rat*
IV 1 mg kg^{-1}	AUC (ng.h/mL)	270	236	151	250
	Vss (L/kg)	0.70	0.54	0.50	1.50
	CL (ml/min/kg)	44.3	42.1	27.5	66.3
	$T_{1/2}$ (h)	0.29	0.31	0.20	0.40

PO 3 mg kg $^{-1}$	T_{max} (h)	0.25	0.25	0.25	0.25
	C_{max} (ng/mL)	368	396	402	129
	AUC (ng.h/mL)	300	219	277	86
	$T_{1/2}$ (h)	0.67	0.80	0.30	0.80
	%F*	**37**	**31**	**15**	**11**

Molecular docking study of 32ao of Series 3

Molecular docking study shows that **32ao** and IBR adopts similar conformation in the in the active site of the BTK enzyme (**Figure 17)**. The pyrimidine ring nitrogen forms an H-bond with the backbone NH of Met477 in the hinge region of the BTK domain, while the amino group of the pyrimidine ring **32ao** forms an H-bond with the backbone carbonyl of Glu474. With the thiol group of Cys481 in BTK, which binds covalently as Michael adducts, both IBR and **32ao** revealed significant interactions. The additional interactions that **32ao** has with Ser538 in the active domain of the BTK enzyme describe its potent BTK inhibitory activity. The docking scores of IBR and **32ao** were -11.08 and -11.62 kcal/mol, respectively.

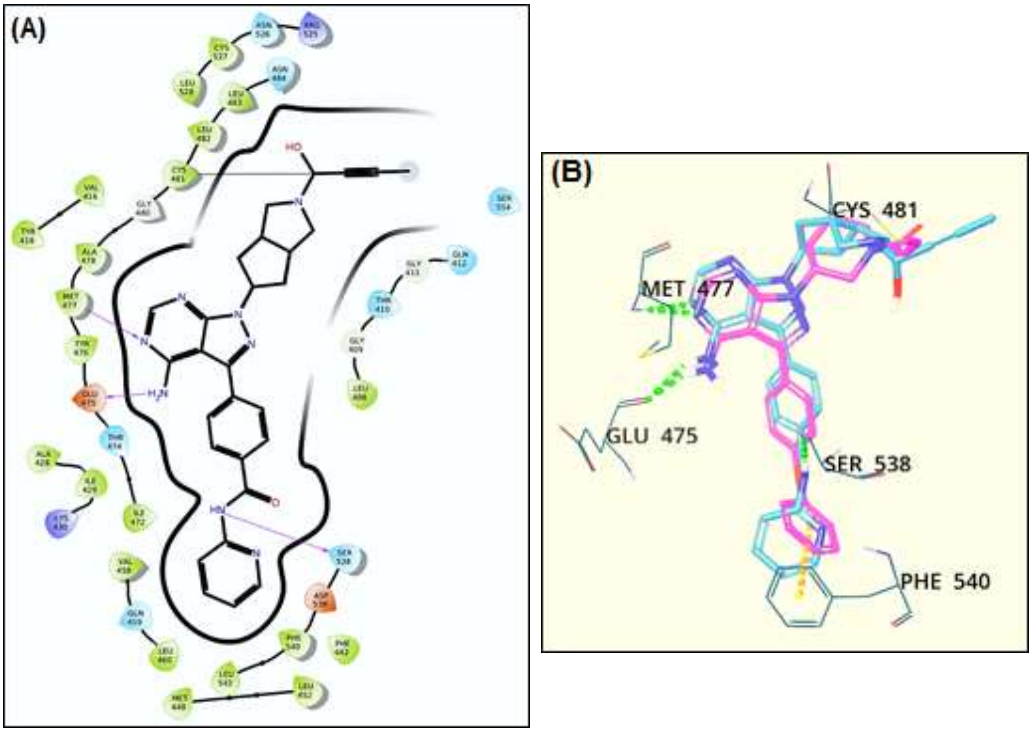

2.5. BTK inhibitors (41, 42, 51, 52, 61, 62, 71, and 72) based on pyrazolo-pyrimidin-4-amine scaffold's mimetic aromatic heterocycles (Series 4)

Pyrazolo-pyrimidine is a key pharmacophore of Pyrazolo-pyrimidin-4-amine-based BTK inhibitors and it interacts with the hinge region of BTK enzyme through the hydrogen bonding. It also provides orientation to the aromatic backbone and linker, which create a "Y" shape that is essential for BTK inhibitory activities. In the present **Series 4**, we intended to incorporate mimetic heterocycles of Pyrazolo-pyrimidine, such as Pyrrolo-pyrimidin, Oxo-purine, Imidazo-pyrazine, and Pyrazole scaffolds, in place of Pyrazolo-pyrimidine. The aromatic backbone of N-2-pyridylbenzamide and the amine linker of octahydrocyclopenta[c]pyrrol were preserved, while acrylamide and butynamide were utilized as a warhead in the **Series 4** to synthesize eight target compounds **(41**, **42**, **51**, **52**, **61**, **62**, **71**, and **72)**, which were evaluated for *in vitro* BTK inhibitory and anti-proliferative activity. The synthetic routes for the target molecules are described in **Schemes 8**, **9**, **10**, **11**, and **12**.

Scheme 4: Synthetic route of 41 and 42 of Series 4

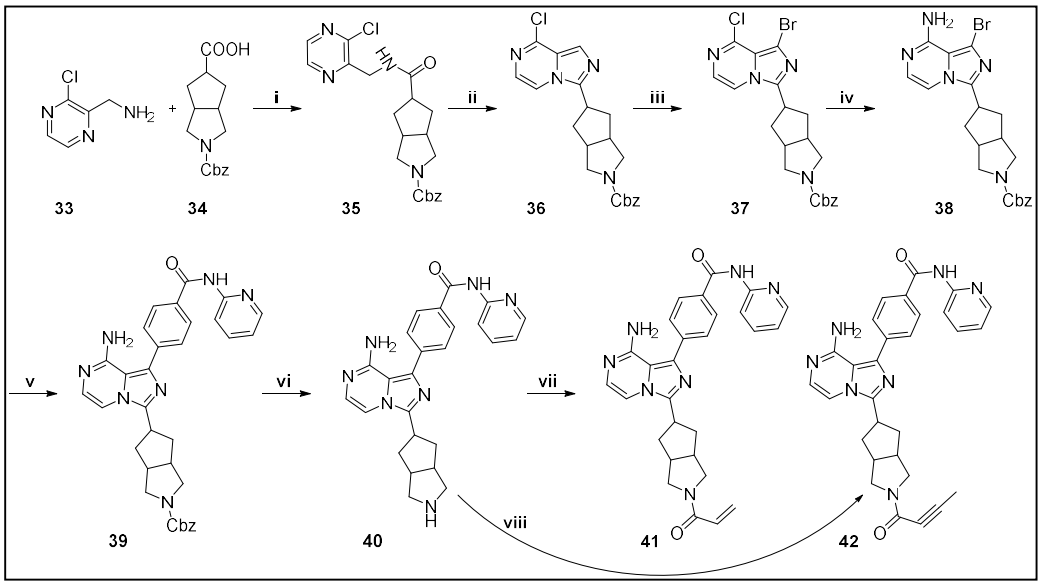

Reagents and conditions: i) O-(1H-Benzotriazol-1-yl)-N,N,N',N'-tetramethyluronium hexafluorophosphate, N,N-Diisopropylethylamine, DMF, 25°C, 16 h, 78%; ii) Phosphorus oxychloride, $DMF_{(cat)}$, ACN, 75 °C, 4 h, 61%; iii) N-bromosuccinimide, DMF, 25°C, 5 h, 89%; iv) Aqueous ammonia, 2-butanol, 90°C, 17 h, 81%; v) (4-(pyridin-2-ylcarbamoyl)phenyl)boronic acid, $PdCl_2(PPh_3)_2$, $KHCO_{3(aq)}$, DMF, 90°C, 8 h, 68%; vi) Pd/C, $H_{2(g)}$, MeOH, 25°C, 2 h, 91%; vii) Acryloyl chloride, N,N-Diisopropylethylamine, DCM, 0°C to 25°C,18 h, 62% viii) but-2-ynoic acid, O-(1H-Benzotriazol-1-yl)-

N,N,N',N'-tetramethyluronium hexafluorophosphate, N,N-Diisopropylethylamine, DMF, 0°C to 25°C, 18 h, 73%.

Scheme 5: Synthetic route of 51 and 52 of Series 4

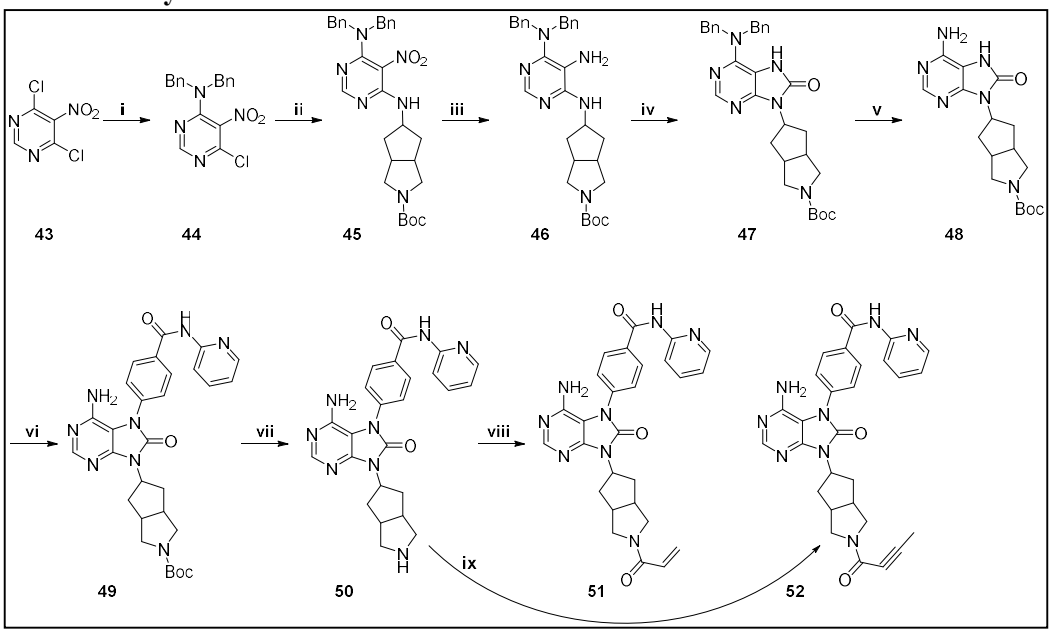

Reagents and conditions: i) Dibenzylamine, DMF, 25°C, 18 h, 85%; ii) Tert-butyl 5-aminohexahydrocyclopenta[c]pyrrole-2(1H)-carboxylate, pyridine, 1,4 dioxane, 80°C, 5 h, 78%; iii) Iron, ammonium chloride, EtOH, H_2O, 80°C, 2 h, 84%; iv) triphosgene, triethylamine, DCM, 25°C, 3 h, 58%; v) Pd/C, $H_{2(g)}$, MeOH, 80%; vi) (4-(pyridin-2-ylcarbamoyl)phenyl)boronic acid, anhydrous copper(II) acetate, pyridine, DCM, 25°C, 48 h, 54%; vii) Trifluoroacetic acid, DCM, 0°C to 25°C, 3 h, 92%; viii) Acryloyl chloride, N,N-Diisopropylethylamine, DCM, 0°C to 25°C, 18 h, 62%; ix) but-2-ynoic acid, O-(1H-Benzotriazol-1-yl)-N,N,N',N'-tetramethyluronium hexafluorophosphate, N,N-Diisopropylethylamine, DMF, 0°C to 25°C, 18 h, 71%.

Scheme 6: Synthetic route of 61 and 62 of Series 4

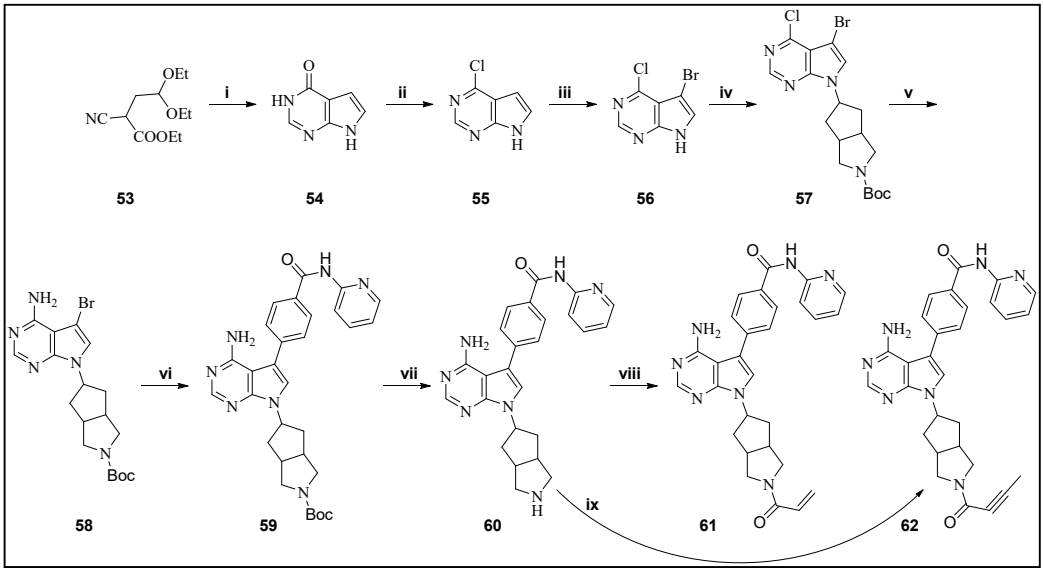

Reagents and conditions: i) Sodium ethoxide, Formamidine acetate, EtOH, 6N $HCl_{(aq)}$, 45°C, 8 h, 54%; ii) Phosphorus oxychloride, 105°C, 2 h, 78%; iii) N-bromosuccinimide, DMF, 25°C, 2 h, 92%; iv) Tert-

butyl 5-((methylsulfonyl)oxy)hexahydrocyclopenta[c]pyrrole-2(1H)-carboxylate, cesium carbonate, DMF, 90ºC, 2 h, 58%.; v) Aqueous ammonia, 1,4 Dioxane, 120ºC, 16 h, 72%; vi) (4-(pyridin-2-ylcarbamoyl)phenyl)boronic acid, $PdCl_2(PPh_3)_2$, $KHCO_{3(aq)}$, DMF, 80ºC, 3 h, 86%; vii) Trifluoroacetic acid, DCM, 25ºC, 5 h, 90%; viii) Acryloyl chloride, N,N-Diisopropylethylamine, DCM, 0°C to 25°C, 18 h, 67%; ix) but-2-ynoic acid, O-(1H-Benzotriazol-1-yl)-N,N,N',N'-tetramethyluronium hexafluorophosphate, N,N-Diisopropylethylamine, DMF, 0°C to 25ºC, 18 h, 65%.

Scheme 7: Synthetic route of 71 and 72 of Series 4

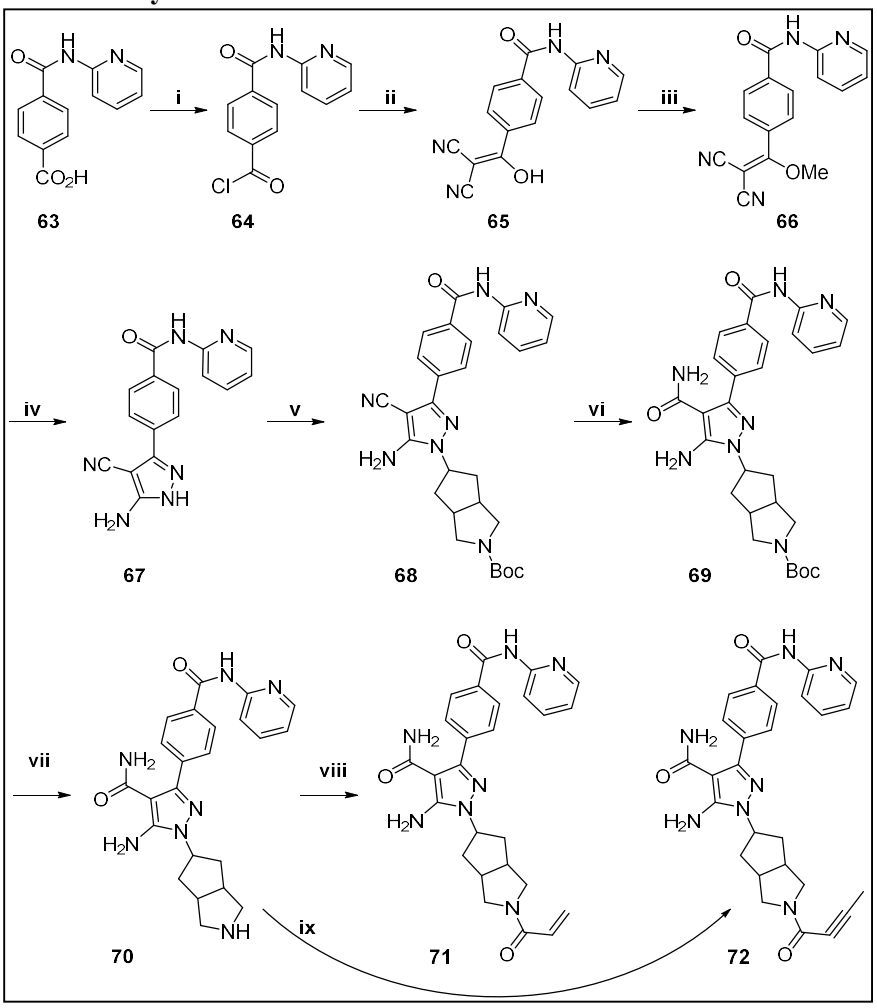

Reagents and conditions: i) Thionyl chloride, 85ºC, 4 h, 99%; ii) Malononitrile, N,N-Diisopropylethylamine, THF, 25ºC, 16 h, 98%; iii) Trimethyl orthoformate, 75ºC, 16 h, 70%; iv) Hydrazine hydrate, EtOH, 25ºC, 16 h, 68%; v) Tert-butyl 5-((methylsulfonyl)oxy)hexahydrocyclopenta[c]pyrrole-2(1H)-carboxylate, cesium carbonate, DMF, 90ºC, 16 h, 59%; vi) Hydrogen peroxide, Potassium carbonate, EtOH, DMSO, 45ºC, 1 h, 65%; vii) Trifluoroacetic acid, DCM, 25ºC, 5 h, 88%; viii) Acryloyl chloride, N,N-Diisopropylethylamine, DCM, 0°C to 25°C, 18 h, 52%; ix) but-2-ynoic acid, O-(1H-Benzotriazol-1-yl)-N,N,N',N'-tetramethyluronium hexafluorophosphate, N,N-Diisopropylethylamine, DMF, 0°C to 25ºC, 18 h, 58%.

Biological evaluation of Series 4

Table 10. ***In vitro*** **BTK enzyme and TMD8 cell proliferation inhibitory data of 41, 42, 51, 52, 61, 62, 71, and 72 of Series 4**

Comp.	Chemical structure	BTK IC_{50} (nM)[a]	TMD8 IC_{50} (nM)[b]	Comp.	Chemical structure	BTK IC_{50} (nM)[a]	TMD8 IC_{50} (nM)[b]
41	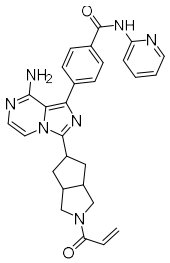	5.4	4.9	**42**	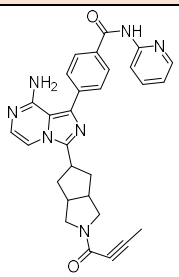	3.6	3.0
51	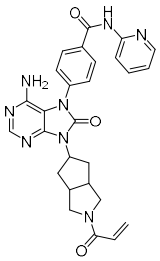	25.1	12.0	**52**	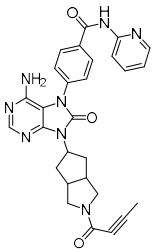	20.2	16.4
61	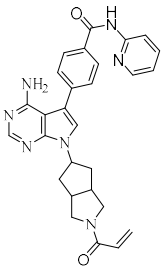	2.4	2.5	**62**	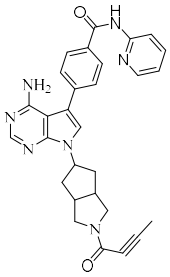	2.9	3.3
71	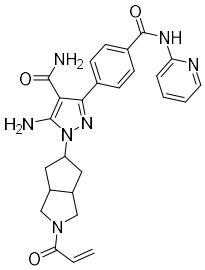	4.3	1.9	**72**	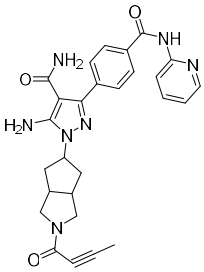	5.1	3.8

Table 11. CYP and hERG inhibitory activity of the lead compound of Series 4

Comp.	%hERG[a] inhibition @ 10 µM	% CYP inhibition[b] @ 10 µM					
		CYP1A2	CYP2C8	CYP2C9	CYP2D6	CYP2C19	CYP3A4
61	**28**	**17**	**57**	**43**	**57**	**7**	**11**
IBR	35	NI	**81**	**86**	31	39	**55**

2.6. Developmental studies of 32b

Several compounds were found to have potent *in vitro* BTK inhibitory and anti-proliferative activity; however, subsequent screening for CYP and hERG liabilities narrowed their number to a few, particularly **24e**, **32b**, and **32ao**. It was discovered that **32b** had a better *in vivo* pharmacokinetic profile than **24e**, **32ao**, and IBR, when the pharmacokinetic profiles of **24e**, **32b**, **32ao**, and IBR (positive control) were evaluated (**Table 4, 7,** and **10**). Moreover, molecular modelling of **32b** validates that it has potent BTK inhibitory activity related to its covalent binding to the BTK enzyme (see section 2.3.3.). Because of its encouraging preliminary biological features, **32b** was adjudged a potential candidate for developmental studies. Wherein **32b** was assessed for biological efficacy studies, comprising anti-tumor activity in the TMD8 xenograft model and anti-arthritic efficacy in the collagen-induced arthritis (CIA) mice model. The covalent binding, kinase selectivity, metabolic stability, permeability, and plasma protein binding of **32b** also were determined. Finally, repeat-dose acute toxicity studies (14 days) in rats were carried out to evaluate the safety profile of **32b**.

ADME profile of 32b

Caco-2 permeability

32b showed low to moderate permeability across the Caco2 cells monolayer and was found to be a substrate of efflux transporters. The apparent permeability (Papp) was 33 nm/sec with an efflux ratio of 5:1.

Metabolic stability

In mouse, rat, dog, and human liver microsomes, **32b** was discovered to be highly to moderately stable, however it was unstable in monkey liver microsomes. **32b** metabolised only up to 13% in mouse liver microsomes (mClint: 0.46 mL/min/g liver), while in rat liver microsomes, 55% of **32b** was metabolised (mClint: 2.62 mL/min/g liver). In dog and human liver microsomes, **32b** was metabolised at rates of 18% (mClint: 0.67 mL/min/g liver) and 32% (mClint: 1.28 mL/min/g liver), respectively. Interestingly, the stability of **32b** was much lower in monkey liver microsomes (66% metabolised with mClint of 3.49 mL/min/g of liver).

Plasma protein binding

32b showed accepted plasma protein binding ability in rat and human plasma (91.2% and 98.4% in rat and human, respectively).

In vivo efficacy studies of 32b

Antitumor activity of 32b in TMD8 xenograft model

To validate the *in vitro* anti-proliferative effect of **32b** in an *in vivo* system, the anti-tumor potential of **32b** was assessed in TMD-8 DLBCL xenograft tumor-bearing mice (see experimental section 4.2.6.1. for detailed protocol). Animals were treated with 1.5, 3, and 15 mg/kg, BID, of **32b** for 20 days via the oral route of administration. The tumour volume was measured as described in the experimental section. **32b** showed dose-dependent tumour growth inhibition (10%,50%, and 88%, respectively). The growth inhibitory property of **32b** was more prominent after 7 days and onwards. We also compared the efficacy of **32b** (12.5 mg/kg) against IBR (12.5 mg/kg) for its antitumor activities. Our results demonstrated that **32b** had slightly better potency compared to IBR at the same dose. It is important to note that **32b** does not have any effect on the body weight of the animals during the 20-day treatment period. Thus, the *in vivo* study validates the antitumor potential of **32b**.

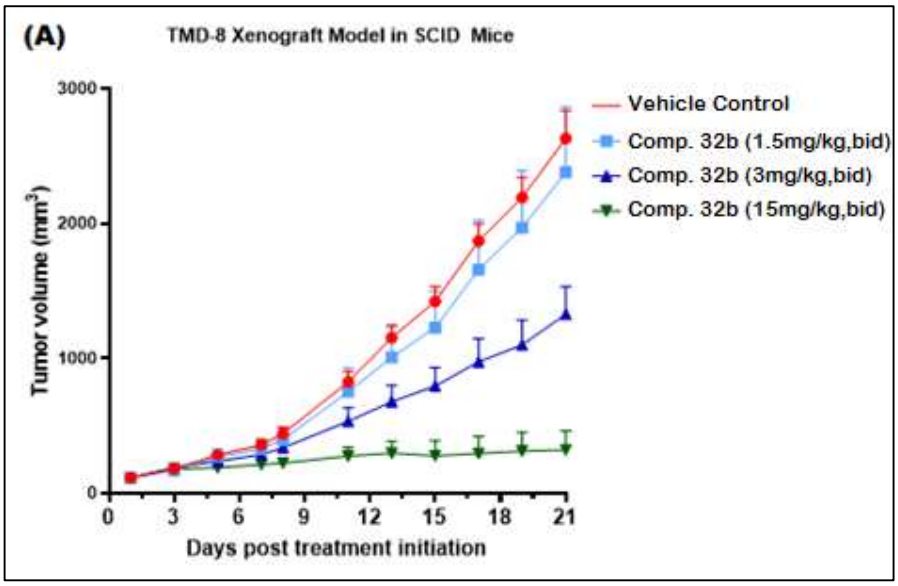
(A)
TMD-8 Xenograft Model in SCID Mice
Tumor volume (mm³)
Days post treatment initiation
Vehicle Control
Comp. 32b (1.5mg/kg,bid)
Comp. 32b (3mg/kg,bid)
Comp. 32b (15mg/kg,bid)

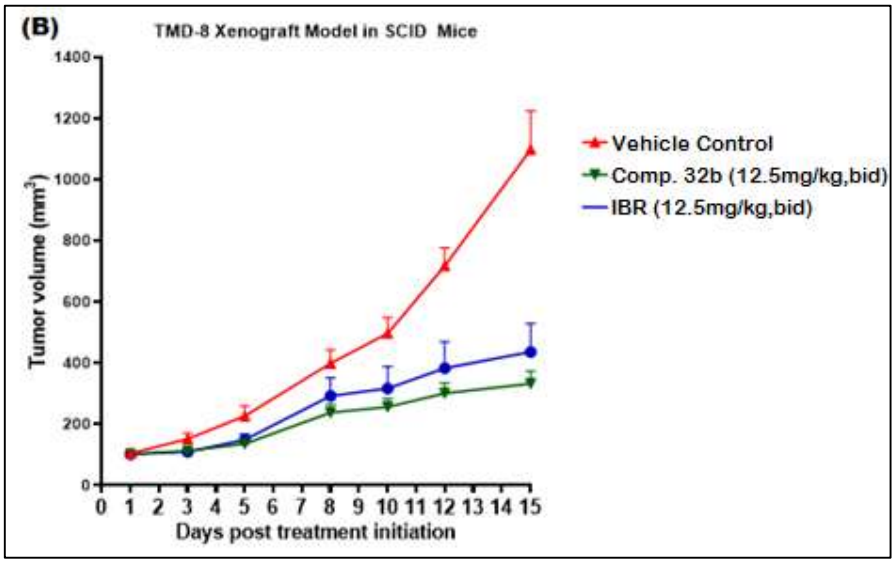
(B)
TMD-8 Xenograft Model in SCID Mice
Tumor volume (mm³)
Days post treatment initiation
Vehicle Control
Comp. 32b (12.5mg/kg,bid)
IBR (12.5mg/kg,bid)

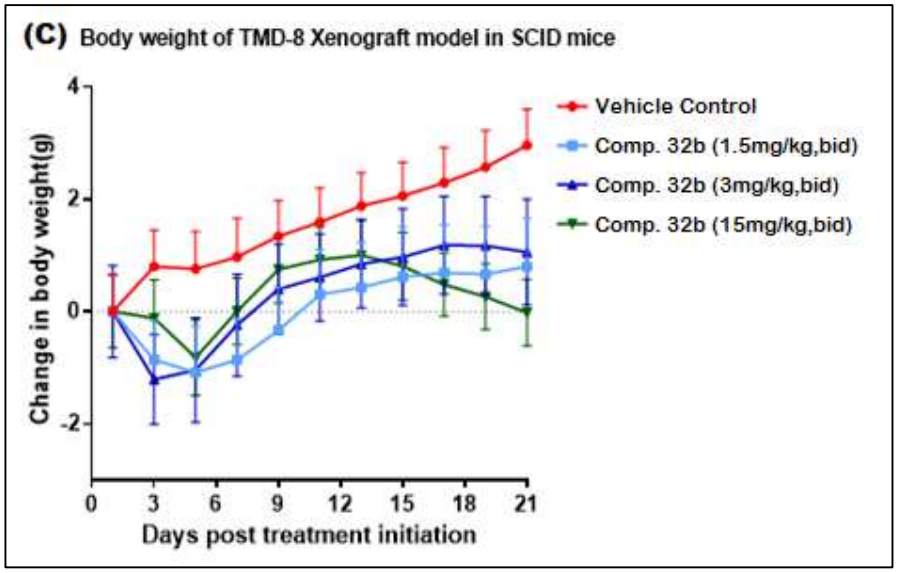
(C) Body weight of TMD-8 Xenograft model in SCID mice
Change in body weight(g)
Days post treatment initiation
Vehicle Control
Comp. 32b (1.5mg/kg,bid)
Comp. 32b (3mg/kg,bid)
Comp. 32b (15mg/kg,bid)

Anti-arthritic efficacy of 32b in a collagen-induced arthritis (CIA) mice model

Arthritis was developed in male DBA1j mice using a collagen mixture, and mice were recruited for the study once clinical signs were visible. Ten animals were assigned to each of the three groups [vehicle, positive control (IBR, 0.6 mg/kg), and test compound **32b** (0.5 mg/kg)]. Treatment was continued for four weeks, once daily, and the percentage inhibition in the clinical score was recorded (see experimental section 4.2.6.2. for detailed protocol). Also, to check dose-dependent anti-arthritic activity, doses of 0.125, 0.25, 0.5, and 1 mg/kg of **32b** were administered orally, once daily, for 28 days. The study results indicated that **32b** was far more *in vivo* efficacious compare to IBR. **32b** (0.5 mg/kg) caused a 93% reduction in clinical score, while IBR (0.6 mg/kg) showed only a 40% reduction in clinical score in the CIA model. **32b** efficacy was found to be dose related, as the reductions in clinical score were 22 %, 61 %, 93 %, and 97 %, per doses of 0.125, 0.25, 0.5, and 1 mg/kg, respectively.

As shown in **Figure**, treatment with **32b** significantly suppressed the progression of disease; 0.25 mg/kg of **32b** once daily was the lowest dose, which showed improvement in clinical signs of disease after two days of initial dosing. The inflammation and damage to the paw were also assessed histologically. Treatment with **32b** displayed a reduction in the paw swelling based on lower histologic severity scores in the **32b** treated groups compared with the vehicle control. The paws from the vehicle-treated control group had a group mean severity of 10.4, while the mean severity scores in the **32b** treated mice were 5, 3.75, 1, and 0.2 at dosages of 0.125, 0.25, 0.5, and 1 mg/kg, respectively. The body weights of the animals were also recorded three times a week as a measure of treatment-related side effects. No changes in the mice's body weight were observed in any treatment group compared to the vehicle control group. Thus, the improved PK of **32b** justifies its potent *in vivo* efficacy in the CIA mice model.

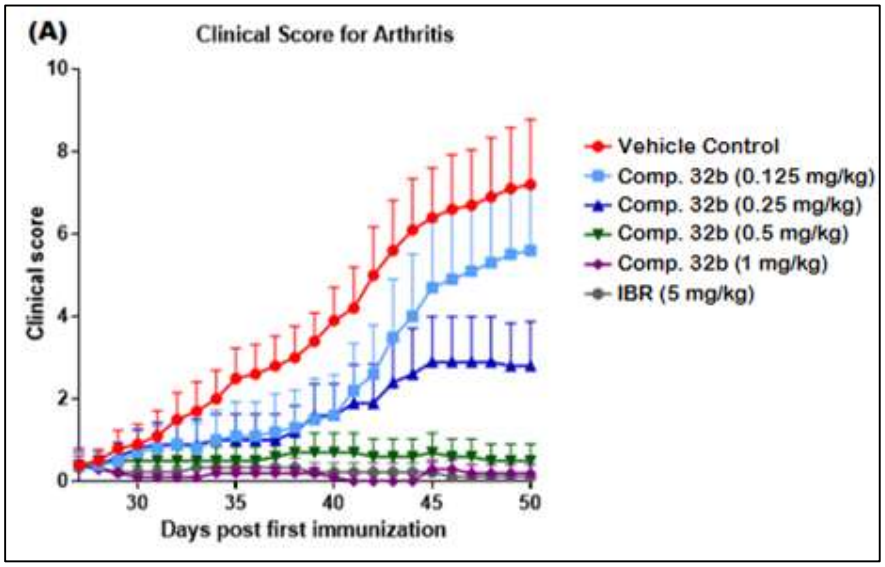
(A)
Clinical Score for Arthritis
Clinical score
Days post first immunization
Vehicle Control
Comp. 32b (0.125 mg/kg)
Comp. 32b (0.25 mg/kg)
Comp. 32b (0.5 mg/kg)
Comp. 32b (1 mg/kg)
IBR (5 mg/kg)

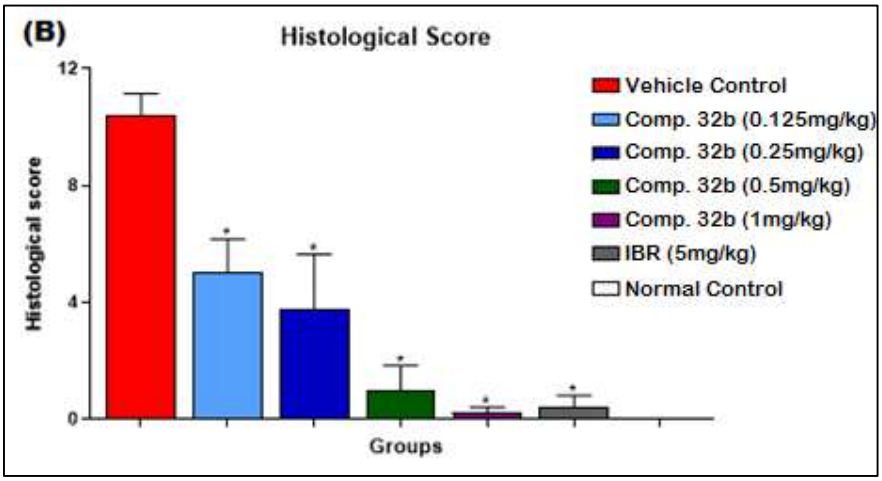
(B)
Histological Score
Histological score
Groups
Vehicle Control
Comp. 32b (0.125mg/kg)
Comp. 32b (0.25mg/kg)
Comp. 32b (0.5mg/kg)
Comp. 32b (1mg/kg)
IBR (5mg/kg)
Normal Control

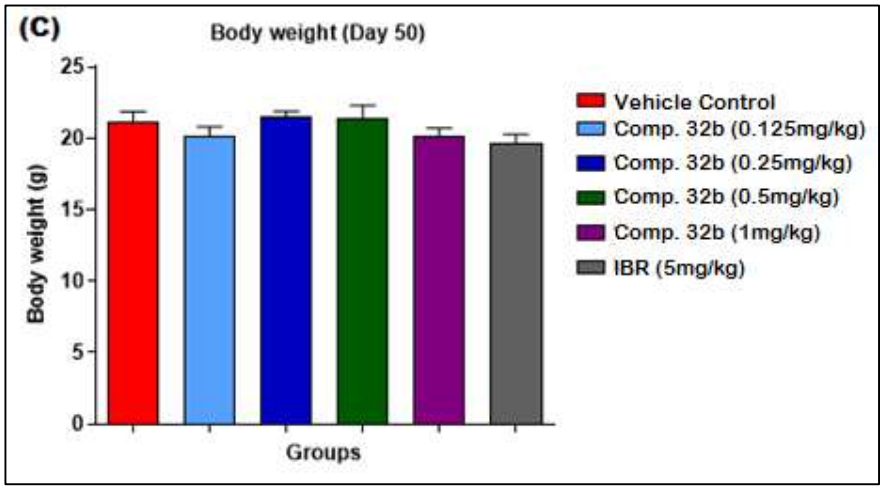
(C)
Body weight (Day 50)
Body weight (g)
Groups
Vehicle Control
Comp. 32b (0.125mg/kg)
Comp. 32b (0.25mg/kg)
Comp. 32b (0.5mg/kg)
Comp. 32b (1mg/kg)
IBR (5mg/kg)

Irreversible (covalent) binding of 32b to the BTK enzyme

To determine that **32b** was irreversibly bonded to the BTK enzyme, we followed the technique described by Honigberg et al. The first FDA-approved BTK inhibitor, IBR, was shown to be covalently bonded to the BTK enzyme by using the mentioned technique. We used fluorescence-tagged IBR (IBR-BFL) in a THP-1 cell-based binding assay. Analysis of the fluorescent gel showed a fluorescent band at 70 kDa, corresponding to the molecular weight of BTK enzyme. The band started appearing at 0.5 μmol/L Ib-BFL and attained saturation at 5 μmol/L and higher concentrations. Immunoblotting of the same gel with anti-BTK Ab confirmed the presence of constant levels of total BTK with increasing concentrations of IB-BFL. This indicated that IB-BFL binds to BTK enzyme, and the binding is detectable at and above 0.5 μmol/L. This step was important to find out the concentration of IB-BFL to be used in our corresponding assays. Since 5 μmol/L of Ib-BFL was saturating the binding, we chose a sub saturating concentration of 2 μmol/L for the following experiment. In order to test whether IBR and **32b** bind to the same site on BTK enzyme, we adopted a competition binding assay. In this assay, THP-1 cells were pre incubated with an increasing concentration of **32b**, followed by incubation with 2 μmol/L of IBR-BFL. **Figure**, clearly showed that IBR-BFL could either replace or occupy free sites at a **32b** concentration lower than 5 μmol/L. However, on increasing the concentration of **32b** to 10 μmol/L and above, the IBR-BFL-BTK interaction was no longer detectable. Since the levels of BTK enzyme did not change, this demonstrated that **32b** binds to the same site as IBR and that the binding is irreversible in nature. A densitometric scan of the fluorescent bands yielded an IC_{50} of 1 nmol/L for this binding.

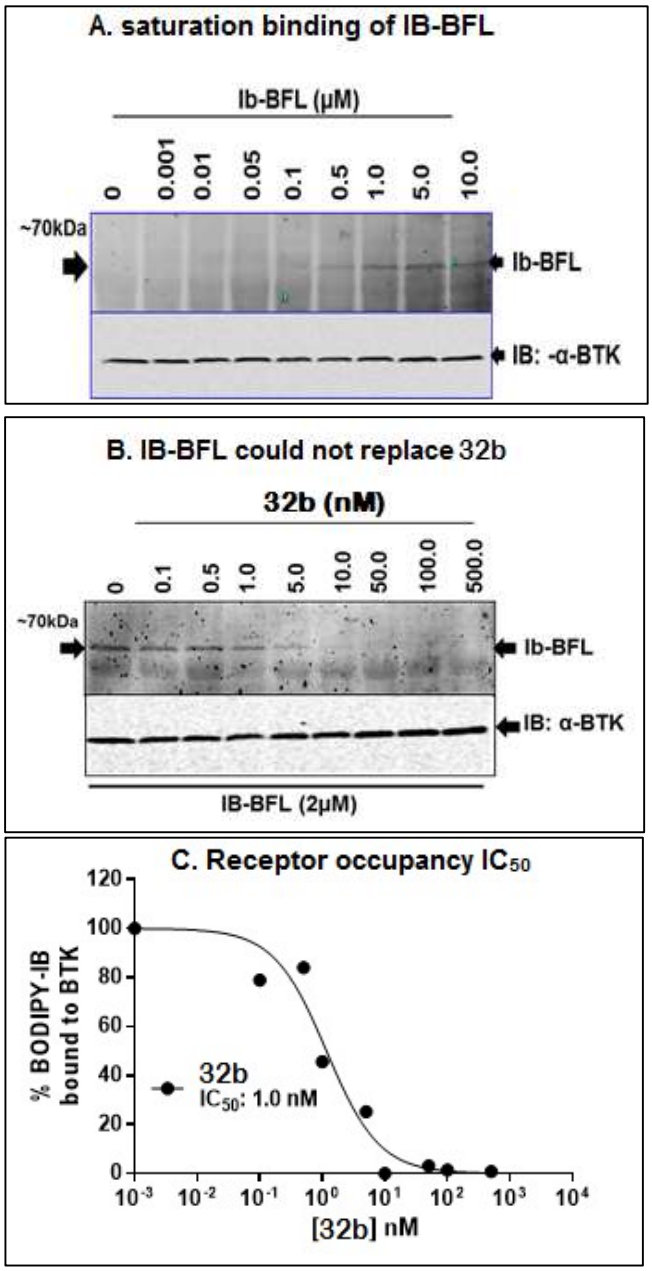

Kinase selectivity of 32b

BTK is among the 11 kinases (TEC, SRC, and EGFR family) having cysteine residues at the structurally equivalent position in the ATP binding domain. For additional profiling studies, **32b** was evaluated for kinase selectivity in a biochemical enzyme inhibition assay, and IC_{50}

values were determined. Screening of a panel of 13 different kinases demonstrated that **32b** is highly selective for BTK and TEC, while for other tyrosine kinases, namely ITK, FGR, HCK, and JAK3, **32b** was found to be 350 times less potent. Overall, **32b** was found to be more BTK and TEC selective.

Table 12. Biochemical kinase selectivity of 32b

Kinases	IC_{50} (µmol/L)[a]
	32b
BTK	0.027-0.041
ITK	18-24
JAK3	>10
TEC	0.025-0.038
ERBB2 wt	1.7-2.3
EGF-R wt	2.3-3.5
BLK	1.1-2.2
BMX	0.091-0.12
ERBB4	0.12-0.19
EGFRT790M	4.2-5.7
FGR	10-13
FRK	1.3-1.7
HCK	>10

Safety profile of 32b

Oral doses were administered to groups of five male and female rats. Once day for 14 days, at doses of 50, 100, and 300 mg/kg of compound **32b**. Considering that the ED_{50} dose was 3 mg/kg as determined by the CIA model studies, these doses are 16x, 33x, and 100x of the ED_{50}, respectively.

To assess the safety profile of **32b**, repeat-dose acute toxicity studies (14 days) were carried out in male Wistar rats, and various parameters such as gross pathology, clinical signs, body weight, organ weight, serum chemistry, and haematological changes were recorded (see experimental section 4.2.10. for detailed protocol). Oral doses were administered to groups of five male and female Wistar rats. Once a day for 14 days, at doses of 50, 100, and 300 mg/kg of compound

32b, considering that the ED_{50} dose was 3 mg/kg as determined by the CIA model, these doses are 16x, 33x, and 100x of the ED_{50}, respectively. Daily oral administration of compound **32b** over a period of 2 weeks did not affect the survival of Wistar rats, and also no adverse changes related to gross pathology, clinical signs, body weight, or feed consumption were noticed, compared to the control group (**Table 14**). As shown in **Tables 15** and **16**, the hematological parameters of compound **32b** were found to be comparable to those of control animals. Similarly, compound **32b** showed no significant changes in the serum hepatotoxicity assessment parameters as compared to the control group. Also, the compound **32b** treated groups showed no changes in the key organ weights such as the heart, kidney, spleen, brain, etc.

Chapter 3. Summery, Conclusion, and Way Forward

In our ongoing quest to discover a novel BTK inhibitor, 64 target compounds were designed and synthesised through four distinct series. In **Series 1**, we have selected eight saturated bicyclic amine analogues for bioisosteric replacement of piperidine in IBR. In **Series 2**, for aromatic backbone optimisation, three sets of aromatic backbone were selected. In the first set of **series 2**, benzamide and picolinamide-based aromatic backbones were selected, whereas in the second set of **series 2**, 4-phenyl ether, 4-phenyl thioether, and 4-phenyl alkyl derivatives were used as aromatic backbones. Phenyl-containing fused heterocycles were enlisted as the aromatic backbone for the third set of **series 2**.

To explore the impact of the warhead on BTK inhibitory activities, conventional warhead acrylamide was swapped with α, β-unsaturated amide in **Series 3**. In **Series 4**, Pyrazolo-pyrimidine, a hinge binder of BTK inhibitors, was replaced with mimetic heterocycles of Pyrazolo-pyrimidine, such as Pyrrolo-pyrimidin, Oxo-purine, Imidazo-pyrazine, and Pyrazole scaffolds.

Analytical data were used to characterise all of the target compounds, which were then evaluated for *in vitro* BTK inhibitory and anti-proliferative activities. Compounds having significant *in vitro* activity were studied for CYP and hERG inhibition, pharmacokinetic properties, and molecular docking. Out of the four series, the most potent molecule **(32b)** was ultimately selected for *in vivo* pharmacological evaluation, such as anti-tumour activity using the TMD8 xenograft model, anti-arthritic efficacy using the CIA mice model, kinase selectivity, an irreversible BTK inhibitory binding study, and acute toxicities studies.

A novel **Series 1** of 3-(4-phenoxyphenyl)-pyrazolo[3,4-d]pyrimidin-4-amine scaffold-based BTK inhibitors (**24a-h**) were synthesised, wherein the linker amine (piperidine) of Ibrutinib (IBR) was replaced with eight saturated bicyclic linker amines. The most efficacious of the set was discovered to be compound **24e (***in vitro* potency was equivalent to IBR). Moreover, **24e** possessed a superior pharmacokinetic profile and was devoid of CYP and hERG liabilities. The significant potency of **24e** was also validated by molecular modelling studies.

In **Series 2**, to optimise the aromatic backbone (phenoxy phenyl) of compound **24e**, a total of forty compounds (**32a–an**) were synthesised. In this series, benzamide and thioether analogues as aromatic backbones demonstrated excellent BTK inhibitory and anti-proliferative activity, particularly **32b**, **32d**, **32e**, **32u**, and **32v**. During subsequent biological evaluation, only compound **32b** was identified to have superior bioavailability and it was found to be devoid of CYP and hERG at 10 μM concentration. Molecular docking revealed that the N-2-pyridyl ring of **32b** exhibits the important π-π interaction and also additional bonding in the catalytic domain of BTK enzyme with Ser538 and Gln412, which was believed to be contributing to its potent BTK inhibitory activity.

To investigate the influence of the warhead on *in vitro* activities in **Series 3**, acrylamide was swapped with specific α, β-unsaturated amide to construct **32ao-av**. butynamide (**32ao**), as the

warhead displayed excellent potency in the BTK enzyme and TMD8 cell proliferation assays, with IC_{50} values of 1.2 nM and 0.9 nM, respectively. **32ao** was found to be free of CYP and hERG liabilities and had a better PK profile than IBR, although **32ao** has a slightly inferior PK profile compared to **32b**.

In the final set (**Series 4**) of compounds (**41, 42, 51, 52, 61, 62, 71,** and **72**), attempts were made to replace the Pyrazolo-pyrimidin-4-amine scaffold with its mimetic aromatic heterocycles, particularly Pyrrolo-pyrimidin, Oxo-purine, Imidazo-pyrazine, and Pyrazole scaffolds. However, none of them were found to be as efficacious as its Pyrazolo-pyrimidin-4-amine counterpart.

In a comparative biological assessment of pharmacokinetics and *in vitro* assays, **32b** was found to be superior and devoid of CYP and hERG. Thus, **32b** was designated for developmental studies.

- The anti-tumor potential of 32b was assessed in TMD-8 xenograft tumor-bearing mice for 20 days via oral administration. The findings revealed that 32b suppressed tumour growth in a dose-dependent manner (10%, 50%, and 88%, respectively), and its growth-inhibitory effects became more prominent after 7 days and onwards.
- 32b was found to be extremely effective in alleviating arthritis, causing a 97% reduction in the clinical score in a collagen-induced arthritis (CIA) mice model. In histological evaluation, treatment with 32b demonstrated a substantial reduction of mice paw swelling as compared to the control group. The histologic severity scores for the mice treated with 32b at dosages of 0.125, 0.25, 0.5, and 1 mg/kg were 5, 3.75, 1, and 0.2, compared to a histologic severity score of 10.4 for the paws from the vehicle-treated control group.
- 32b has been found to be BTK selective and covalently binds to the BTK enzyme.

- At doses up to 300 mg/kg (100x of the ED_{50}), 32b exhibited an ideal preclinical safety profile, with no negative effects seen in rats.

In summary, the pre-clinical profile of **32b** indicates that the new class of BTK inhibitor could be a viable therapeutic option for the treatment of autoimmune diseases like cancer and rheumatoid arthritis.

Future plan for 32b

Additional profiling studies will be carried out with **32b**, such as single and repeated dose PK studies in higher species (dogs or primates), including chronic toxicity studies in higher animal species. If **32b** fulfils pre-clinical candidate selection criteria, it will be subjected to IND enabling studies.

Overall project outcome

Rational designing and synthesis of novel BTK inhibitors, SAR generation, *in vitro*, and *in vivo* profiling of lead compounds resulted in a novel BTK inhibitor **(32b)** in the present investigation. Overall, **32b** looks like a promising candidate in terms of efficacy and safety margin in acute animal studies. If our initial observations translate into chronic animal studies, **32b** may turn out to be a safe and efficacious BTK inhibitor for the treatment of various autoimmune disorders such as RA and cancer.

Bibliography and Webliography

1. Ubersax JA, Ferrell JE Jr. Mechanisms of specificity in protein phosphorylation. Nat Rev Mol Cell Biol. 2007, 8(7), 530-41.

2. Cohen P. Protein kinases-the major drug targets of the twenty-first century. Nat Rev Drug Discov. 2002, 1(4), 309-15.

3. Holzer H, Duntze W. Annual Review of Biochemistry, 1971, 40, 345-374.

4. Heath CM, Stahl PD, Barbieri MA. Lipid kinases play crucial and multiple roles in membrane trafficking and signaling. Histology and Histopathology. 2003, 18(3), 989–998.

5. Khan WN, Alt FW, Gerstein RM, Malynn BA, Larsson I, Rathbun G, Davidson L, Muller S, Kantor AB, Herzenberg LA, et al. Defective B cell development and function in BTK-deficient mice. Immunity. 1995, 3, 283–99.

6. Bolen JB. Protein tyrosine kinases in the initiation of antigen receptor signaling. Curr Opin Immunol. 1995, 7(3), 306-11.

7. Mano H. Tec family of protein-tyrosine kinases: an overview of their structure and function. Cytokine Growth Factor Rev. 1999,10(3-4), 267-80.

8. August A, Sadra A, Dupont B, Hanafusa H. Src-induced activation of inducible T cell kinase (ITK) requires phosphatidylinositol 3-kinase activity and the Pleckstrin homology domain of inducible T cell kinase. Proc Natl Acad Sci U S A. 1997, 94(21), 11227-32.

9. Salim K, Bottomley MJ, Querfurth E, Zvelebil MJ, Gout I, Scaife R, et al. Distinct specificity in the recognition of phosphoinositide by the pleckstrin homology domains of dynamine and Bruton's tyrosine kinase. EMBO J. 1996, 15(22), 6241-50.

10. Jiang Y, Ma W, Wan Y, Kozasa T, Hattori S, Huang XY. The G protein G alpha12 stimulates Bruton's tyrosine kinase and a rasGAP through a conserved PH/BM domain. Nature. 1998, 395(6704), 808-13.

11. Tsukada S, Simon MI, Witte ON, Katz A. Binding of beta gamma subunits of heterotrimeric G proteins to the PH domain of Bruton tyrosine kinase. Proc Natl Acad Sci U S A. 1994, 91(23), 11256-60.

12. Hyvonen M, Saraste M. Structure of the PH domain and BTK motif from Bruton's tyrosine kinase: molecular explanations for X-linked agammaglobulinaemia. EMBO J. 1997, 16(12), 3396-404.

13. Rawlings DJ, Scharenberg AM, Park H, Wahl MI, Lin S, Kato RM, et al. Activation of BTK by a phosphorylation mechanism initiated by SRC family kinases. Science. 1996, 271(5250), 822-5.

14. Andreotti AH, Bunnell SC, Feng S, Berg LJ, Schreiber SL. Regulatory intramolecular association in a tyrosine kinase of the Tec family. Nature. 1997, 385(6611), 93-7.

15. Yamashita Y, Miyazato A, Ohya K, Ikeda U, Shimada K, Miura Y, et al. Deletion of Src homology 3 domain results in constitutive activation of Tec protein-tyrosine kinase. Jpn J Cancer Res. 1996, 87(11), 1106-10.

16. Backesjo CM, Vargas L, Superti-Furga G, Smith CI. Phosphorylation of Bruton's tyrosine kinase by c-Abl. Biochem Biophys Res Commun. 2002, 299(3), 510-5.

17. Guinamard R, Aspenstrom P, Fougereau M, Chavrier P, Guillemot JC. Tyrosine phosphorylation of the Wiskott-Aldrich syndrome protein by Lyn and BTK is regulated by CDC42. FEBS Lett. 1998. 434(3), 431-6.

18. Guinamard R, Fougereau M, Seckinger P. The SH3 domain of Bruton's tyrosine kinase interacts with Vav, Sam68 and EWS. Scand J Immunol. 1997, 45(6):587-95.

19. Park H, Wahl MI, Afar DE, Turck CW, Rawlings DJ, Tam C, et al. Regulation of BTK function by a major autophosphorylation site within the SH3 domain. Immunity. 1996, 4(5), 515-25.

20. Ohya K, Kajigaya S, Kitanaka A, Yoshida K, Miyazato A, Yamashita Y, et al. Molecular cloning of a docking protein, BRDG1, that acts downstream of the Tec tyrosine kinase. Proc Natl Acad Sci U S A. 1999, 96(21), 11976-81.

21. Oppermann FS, Gnad F, Olsen JV, Hornberger R, Greff Z, Keri G, et al. Large-scale proteomics analysis of the human kinome. Mol Cell Proteomics. 2009, 8(7), 1751-64.

22. Murphy K. Janeway's Immunobiology (8th ed.). 2012, New York, Garland Science.

23. Alberts B, Johnson A, Lewis J, Raff M, Roberts K, Walter P. B Cells and Antibodies. Molecular Biology of the Cell (4th ed.), 2002.

24. Althwaiqeb SA, Bordoni B. Histology, B Cell Lymphocyte. 2022, StatPearls [Internet], Treasure Island (FL), StatPearls Publishing.

25. Chapman J, Zhang Y. Histology, Hematopoiesis. 2022, StatPearls [Internet], Treasure Island (FL), StatPearls Publishing.

26. Null M, Arbor TC, Agarwal M. Anatomy, Lymphatic System. 2023, StatPearls [Internet], Treasure Island (FL), StatPearls Publishing.

27. Ozdowski L, Gupta V. Physiology, Lymphatic System. 2022, StatPearls [Internet], Treasure Island (FL), StatPearls Publishing.

28. Aziz M, Iheanacho F, Hashmi MF. Physiology, Antibody. 2022, StatPearls [Internet], Treasure Island (FL), StatPearls Publishing.

29. Justiz Vaillant AA, Jamal Z, Patel P, Ramphul K. Immunoglobulin. 2022, StatPearls [Internet], Treasure Island (FL), StatPearls Publishing.

30. Tanaka S, Baba Y. B Cell Receptor Signaling. Adv Exp Med Biol. 2020,1254, 23-36.

31. Grubbs H, Kahwaji CI. Physiology, Active Immunity. 2022, StatPearls [Internet], Treasure Island (FL), StatPearls Publishing.

32. Sauls RS, McCausland C, Taylor BN. Histology, T-Cell Lymphocyte. 2022, StatPearls [Internet], Treasure Island (FL), StatPearls Publishing.

33. Allen HC, Sharma P. Histology, Plasma Cells. 2022, StatPearls [Internet], Treasure Island (FL), StatPearls Publishing.

34. David J. Rawlings et al., Mutation of Unique Region of Bruton's Tyrosine Kinase in Immunodeficient XID Mice. Science, 1993, 261,358-361.

35. Hashimoto A, Okada H, Jiang A, Kurosaki M, Greenberg S, Clark EA, Kurosaki T. Involvement of guanosine triphosphatase and phospholipase C-gamma2 in extracellular signal-regulated kinase, c-Jun NH2-terminal kinase, and p38 mitogen-activated protein kinase activation by the B cell antigen receptor. J Exp Med. 1998, 188, 1287–95.

36. Reth M. Antigen receptor tail clue. Nature. 1989, 338(6214), 383-4.

37. O'Rourke LM, Tooze R, Turner M, Sandoval DM, Carter RH, Tybulewicz VL, Fearon DT. CD19 as a membrane-anchored adaptor protein of B lymphocytes: costimulation of lipid and protein kinases by recruitment of Vav. Immunity. 1998, 8, 635–45.

38. Okada T, Maeda A, Iwamatsu A, Gotoh K, Kurosaki T. BCAP: the tyrosine kinase substrate that connects B cell receptor to phosphoinositide 3-kinase activation. Immunity. 2000,13, 817–27.

39. Saito K, Scharenberg AM, Kinet JP. Interaction between the BTK PH domain and phosphatidylinositol-3,4,5-trisphosphate directly regulates BTK. J Biol Chem. 2001,276, 16201–6.

40. Engels N, Konig LM, Heemann C, Lutz J, Tsubata T, Griep S, Schrader V, Wienands J. Recruitment of the cytoplasmic adaptor Grb2 to surface IgG and IgE provides antigen receptor-intrinsic co stimulation to class-switched B cells. Nat Immunol. 2009, 10, 1018-25.

41. Kim YJ, Sekiya F, Poulin B, Bae YS, Rhee SG. Mechanism of B-cell receptor-induced phosphorylation and activation of phospholipase C-gamma2. Mol Cell Biol. 2004, 24, 9986–99.

42. Petro JB, Rahman SM, Ballard DW, Khan WN. Bruton's tyrosine kinase is required for activation of I kappaβ kinase and nuclear factor kappaβ in response to B cell receptor engagement. J Exp Med. 2000, 191, 1745–54.

43. Bajpai UD, Zhang K, Teutsch M, Sen R, Wortis HH. Bruton's tyrosine kinase links the B cell receptor to nuclear factor kappaβ activation. J Exp Med. 2000, 191, 1735–44.

44. Manning BD, Toker A. AKT/PKB signaling: navigating the network. Cell. 2017, 169, 381–405.

45. Craxton A, Jiang A, Kurosaki T, Clark EA. Syk and Bruton's tyrosine kinase are required for B cell antigen receptor-mediated activation of the kinase Akt. J Biol Chem. 1999, 274, 30644–50.

46. Engels N, Konig LM, Schulze W, Radtke D, Vanshylla K, Lutz J, Winkler TH, Nitschke L, Wienands J. The immunoglobulin tail tyrosine motif upgrades memory-type BCRs by incorporating a Grb2-Btk signalling module. Nat Commun. 2014, 5, 5456.

47. Ritter SL, Hall RA. Fine-tuning of GPCR activity by receptor-interacting proteins. Nat Rev Mol Cell Biol. 2009, 10, 819–30.

48. Okada T, Ngo VN, Ekland EH, Forster R, Lipp M, Littman DR, Cyster JG. Chemokine requirements for B cell entry to lymph nodes and Peyer's patches. J Exp Med. 2002, 196, 65–75.

49. Servant G, Weiner OD, Herzmark P, Balla T, Sedat JW, Bourne HR. Polarization of chemoattractant receptor signalling during neutrophil chemotaxis. Science. 2000, 287, 1037–40.

50. Lowry WE, Huang XY, Protein G. Beta gamma subunits act on the catalytic domain to stimulate Bruton's agammaglobulinemia tyrosine kinase. J Biol Chem. 2002, 277, 1488–92.

51. Tsukada S, Simon MI, Witte ON, Katz A. Binding of beta gamma subunits of hetero trimeric G proteins to the PH domain of Bruton tyrosine kinase. Proc Natl Acad Sci U S A. 1994, 91, 11256–60.

52. Bence K, Ma W, Kozasa T, Huang XY. Direct stimulation of Bruton's tyrosine kinase by G(q)-protein alpha-subunit. Nature. 1997, 389, 296–9.

53. de Gorter DJ, Beuling EA, Kersseboom R, Middendorp S, van Gils JM, Hendriks RW, Pals ST, Spaargaren M. Bruton's tyrosine kinase and phospholipase Cgamma2 mediate chemokine-controlled B cell migration and homing. Immunity. 2007, 26, 93–104.

54. Rawlings DJ, Schwartz MA, Jackson SW, Meyer-Bahlburg A. Integration of B cell responses through toll-like receptors and antigen receptors. Nat Rev Immunol. 2012, 12, 282–94.

55. Jefferies CA, Doyle S, Brunner C, Dunne A, Brint E, Wietek C, Walch E, Wirth T, O'Neill LA. Bruton's tyrosine kinase is a toll/interleukin-1 receptor domain binding protein that participates in nuclear factor kappaβ activation by toll like receptor 4. J Biol Chem. 2003;278:26258–64.

56. Liu X, Zhan Z, Li D, Xu L, Ma F, Zhang P, Yao H, Cao X. Intracellular MHC class II molecules promote TLR-triggered innate immune responses by maintaining activation of the kinase BTK. Nat Immunol. 2011, 12, 416–24.

57. Gray P, Dunne A, Brikos C, Jefferies CA, Doyle SL, O'Neill LA. MyD88 adapter like (mal) is phosphorylated by Bruton's tyrosine kinase during TLR2 and TLR4 signal transduction. J Biol Chem. 2006, 281, 10489–95.

58. Nimmerjahn F, Ravetch JV. Fc gamma receptors as regulators of immune responses. Nat Rev Immunol. 2008, 8, 34–47.

59. Bournazos S, Wang TT, Ravetch JV. The role and function of Fc gamma receptors on myeloid cells. Microbiol Spectr. 2016, 4.

60. Kawakami Y, Yao L, Miura T, Tsukada S, Witte ON, Kawakami T. Tyrosine phosphorylation and activation of Bruton tyrosine kinase upon fc epsilon RI cross-linking. Mol Cell Biol. 1994, 14, 5108–13.

61. Justiz Vaillant AA, Stang CM. Lymphoproliferative Disorders. 2022, StatPearls [Internet], Treasure Island (FL), StatPearls Publishing.

62. Justiz Vaillant AA, Ramphul K. Antibody Deficiency Disorder. 2022, StatPearls [Internet], Treasure Island (FL), StatPearls Publishing.

63. Kumar V, Abbas AK, Aster Robbins JC. Diseases of white blood cells, lymph nodes, spleen, and thymus. Robbins and Cotran Pathologic Basis of Disease. 9th ed. Philadelphia, Elsevier. 2015, 579-628.

64. Davis S. Nutritional factors and the development of non-Hodgkin's lymphoma: A review of the evidence. Cancer Research. 1992, 52, 5492s-5495s.

65. Paltiel O, Schmit T, Adler B, et al. The incidence of lymphoma in first-degree relatives of patients with Hodgkin's disease and non-Hodgkin's lymphoma: Results and limitations of a registry-linked study. Cancer. 2000, 88, 2357-2366.

66. Scherr PA, Hutchison GB, Neiman RS. Non-Hodgkin's lymphoma and occupational exposure. Cancer Research. 1992, 52, 5503s-5509s.

67. Vineis P, Faggiano F, Tedeschi M, et al. Incidence rates of lymphomas and soft-tissue sarcomas and environmental measurements of phenoxy herbicides. Journal of the National Cancer Institute. 1991, 83, 362-363.

68. Zahm SH, Blair A. Pesticides and non-Hodgkin's lymphoma. Cancer Research. 1992, 52, 5485s-5488s.

69. Correa A, Jackson L, Mohan A, et al. Use of hair dyes, hematopoietic neoplasms, and lymphomas: A literature review. II. Lymphomas and multiple myeloma. Cancer Investigation. 2000, 18, 467-479.

70. Swerdlow SH, Campo E, Harris NL, et al. WHO Classification of Tumours of Haematopoietic and Lymphoid Tissues. 5th ed. Lyon, IARC, 2017, 189-342.

71. Kridel R, Sehn LH, Gascoyne RD. Pathogenesis of follicular lymphoma. The Journal of Clinical Investigation. 2012, 122, 3424.

72. Roulland S, Kelly RS, Morgado E, et al. t(14; 18) translocation: A predictive blood biomarker for follicular lymphoma. Journal of Clinical Oncology. 2014, 32(13), 1347-1355.

73. Jares P, Colomer D, Campo E. Molecular pathogenesis of mantle cell lymphoma. The Journal of Clinical Investigation. 2012, 122(10), 3416-3423.

74. Swerdlow SH, Kuzu I, Dogan A, et al. The many faces of small B cell lymphomas with plasmacytic differentiation and the contribution of MYD88 testing. Virchows Archiv. 2016,468(3), 259-275.

75. Hamadeh F, MacNamara SP, Aguilera NS, Swerdlow SH, Cook JR. MYD88 L265P mutation analysis helps define nodal lymphoplasmacytic lymphoma. Modern Pathology. 2015, 28(4), 564-574.

76. Molyneux EM, Rochford R, Griffin B, et al. Burkitt's lymphoma. Lancet. 2012, 379, 1234.

77. Love C, Sun Z, Jima D, et al. The genetic landscape of mutations in Burkitt lymphoma. Nature Genetics. 2012, 44(12), 1321-1325.

78. Dave SS, Fu K, Wright GW, et al. Lymphoma/Leukemia Molecular Profiling Project. Molecular diagnosis of Burkitt's lymphoma. The New England Journal of Medicine. 2006, 354(23), 2431-2442.

79. Swerdlow SH. Diagnosis of 'double hit' diffuse large B-cell lymphoma and B-cell lymphoma, unclassifiable, with features intermediate between DLBCL and Burkitt

lymphoma: When and how, FISH versus IHC. Hematology, American Society of Hematology. 2014, 2014(1), 90-99.

80. Yelin E. Work disability in rheumatic diseases. Curr Opin Rheumatol. 2007, 19 (2), 91-96.

81. McInnes, IB, Schett DG. Cytokines in the pathogenesis of rheumatoid arthritis. Nat Rev Immunol. 2007, 7(6), 429-442.

82. Choy EH, Panayi GS. Cytokine pathways and joint inflammation in rheumatoid arthritis. N Engl J Med. 2001, 344(12), 907-916.

83. Lundberg KS, Nijenhuis ER, Vossenaar K, Palmblad WJ, van Venrooij L, Klareskog AJ, Zendman HE. Citrullinated proteins have increased immunogenicity and arthritogenicity and their presence in arthritic joints correlates with disease severity. Arthritis Res Ther. 2005, 7(3), R458-467.

84. www.news-medical.net/health/Rheumatoid-Arthritis-History.aspx.

85. Gomez-Puerta JA, Mócsai A. Tyrosine kinase inhibitors for the treatment of rheumatoid arthritis. Curr Top Med Chem. 2013, 13(6), 760-73.

86. Arneson LC, Carroll KJ, Ruderman EM. Bruton's Tyrosine Kinase Inhibition for the Treatment of Rheumatoid Arthritis. Immunotargets Ther. 2021, 10, 333-342.

87. Sabour J. B-Cell Lymphoma Treatment Options. Published online on March 07, 2022. https://www.verywellhealth.com/b-cell-lymphoma-treatment.

88. Hendriks, R. W.; Yuvaraj, S.; Kil, L. P. Nat. Rev. Cancer 2014, 14, 219–232.

89. Whang, J. A.; Chang, B. Y. Drug Discov. Today 2014, 19, 1200–1204.

90. de Weers M, Verschuren MC, Kraakman EM, Mensink RG, Schuurman RK, van Dongen JJ, Hendriks RW. Eur. J. Immunol. 1993, 23, 3109–3114.

91. Katz FE, Lovering RC, Bradley LA, Rigley KP, Brown D, Cotter F, Chessells JM, Levinsky RJ, Kinnon C. Leukemia. 1994, 8, 574–577.

92. Davis RE, Ngo VN, Lenz G, Tolar P, Young RM, Romesser PB, Kohlhammer H, Lamy L, Zhao H, Yang Y, Xu W, Shaffer AL, Wright G, Xiao W, Powell J, Jiang J, Thomas CJ, Rosenwald A, Ott G, Muller-Hermelink HK, Gascoyne RD, Connors JM, Johnson NA, Rimsza LM, Campo E, Jaffe ES, Wilson WH, Delabie J, Smeland EB, Fisher RI, Braziel RM, Tubbs RR, Cook JR, Weisenburger DD, Chan WC, Pierce SK, Staudt LM. Nature. 2010, 463, 88–92.

93. Hendriks RW, Bredius RG, Pike-Overzet K, Staal FJ. Biology and novel treatment options for XLA, the most common monogenetic immunodeficiency in man. Expert Opin. Ther. Targets. 2011, 15, 1003–1021.

94. Honigberg LA, Smith AM, Sirisawad M, Verner E, Loury D, Chang B, Li S, Pan Z, Thamm DH, Miller RA, Buggy JJ. The Bruton tyrosine kinase inhibitor PCI-32765 blocks B-cell activation and is efficacious in models of autoimmune disease and B-cell malignancy. Proc. Natl. Acad. Sci. U. S. A. 2010, 107(29), 13075–13080.

95. Xu D, Kim Y, Postelnek J, Vu MD, Hu DQ, Liao C, Bradshaw M, Hsu J, Zhang J, Pashine A, Srinivasan D, Woods J, Levin A, O'Mahony A, Owens TD, Lou Y, Hill RJ, Narula S, deMartino J, Fine JS. RN486, a selective Bruton's tyrosine kinase inhibitor, abrogates immune hypersensitivity responses and arthritis in rodents. J. Pharmacol. Exp. Ther. 2012, 341(1), 90–103.

96. Di Paolo JA, Huang T, Balazs M, Barbosa J, Barck KH, Bravo BJ, Carano RAD, Darrow J, Davies DR, DeForge LE, Diehl L, Ferrando R, Gallion SL, Giannetti AM, Gribling P, Hurez V, Hymowitz SG, Jones R, Kropf JE, Lee WP, Maciejewski PM, Mitchell SA, Rong H, Staker BL, Whitney JA,Yeh S, Young WB, C. Yu, J. Zhang, K. Reif, K.S. Currie, Specific BTK inhibition suppresses B cell– and myeloid cell–mediated arthritis, Nat. Chem. Biol. 2011, 7(1), 41–50.

97. Rankin AL, Seth N, Keegan S, Andreyeva T, Cook TA, Edmonds J, Mathialagan N, Benson MJ, Syed J, Zhan Y, Benoit SE, Miyashiro JS, Wood N, Mohan S, Peeva E, Ramaiah SK, Messing D, Homer BL, Dunussi- Joannopoulos K, Nickerson-Nutter CL, Schnute ME, Douhan J. Selective inhibition of BTK prevents murine lupus and antibody-mediated glomerulonephritis. J. Immunol. 2013, 191(9) 4540–4550.

98. Gillooly KM, Pulicicchio C, Pattoli MA, Cheng L, Skala S, Heimrich EM, McIntyre KW, Taylor TL, Kukral DW, Dudhgaonkar S, Nagar J, Banas D, Watterson SH, Tino JA, Fura A, Burke JR, Reddy SV. Bruton's tyrosine kinase Inhibitor BMS-986142 in experimental models of rheumatoid arthritis enhances efficacy of agents representing clinical standard-of-care. PLoSOne. 2017, 12(7), e0181782.

99. Crawford JJ, Johnson AR, Misner DL, Belmont LD, Castanedo G, Choy R, Coraggio M, Dong L, Eigenbrot C, Erickson R, Ghilardi N, Hau J, Katewa A, Kohli PB, Lee W, Lubach JW, McKenzie BS, Ortwine DF, Schutt L, Tay S, Wei B, Reif K, Liu L, Wong H, Young WB. Discovery of GDC-0853: a potent, selective, and non-covalent Bruton's tyrosine kinase inhibitor in early clinical development. J. Med. Chem. 2018, 61, 2227-2245.

100. Haselmayer P, Camps M, Liu-Bujalski L, Nguyen N, Morandi F, Head J, O'Mahony A, Zimmerli SC, Bruns L, Bender AT, Schroeder P, Grenningloh R. Efficacy and pharmacodynamic modeling of the BTK Inhibitor Evobrutinib in autoimmune disease models. J. Immunol. 2019, 202. 2888–2906.

101. Molina-Cerrillo J, Alonso-Gordoa T, Gajate P, Grande E. Bruton's tyrosine kinase (BTK) as a promising target in solid tumors. Cancer Treatment Reviews. 2017, 58, 41.

102. De CS, Kurian J, Dufresne C, Mittermaier AK, Moitessier N. Covalent inhibitors design and discovery. European Journal of Medicinal Chemistry. 2017, 138, 96-114.

103. Pan Z, Scheerens H, Li SJ, Schultz BE, Sprengeler PA, Burrill LC, Mendonca RV, Sweeney MD, Scott KC, Grothaus PG, Jeffery DA, Spoerke JM, Honigberg LA, Young PR, Dalrymple SA, Palmer JT. Discovery of selective irreversible inhibitors for Bruton's tyrosine kinase. ChemMedChem. 2007, 2(1), 58–61.

104. US Food and Drug Administration. Approved Drugs: Ibrutinib. Available at: https://wayback.archiveit.org/7993/20170111231706, http://www.fda.gov/Drugs /Information OnDrugs /ApprovedDrugs/ucm374857.htm.

105. De Vries R, Smit JW, Hellemans P, Jiao J, Murphy J, Skee D, Snoeys J, Sukbuntherng J, Vliegen M, De Zwart L, Mannaert E, De Jong J. Stable isotopelabelled intravenous microdose for absolute bioavailability and effect of grapefruit juice on ibrutinib in healthy adults. Br. J. Clin. Pharmacol. 2016, 81(2),235–245.

106. Eisenmann ED, Fu Q, Muhowski EM, Jin Y, Uddin ME, Garrison DA, Weber RH, Woyach JA, Byrd JC, Sparreboom A, Baker SD, Intentional Modulation of Ibrutinib Pharmacokinetics through CYP3A Inhibition. Cancer Research Communications. 2021, 1(2), 79–89.

107. Furman RR, Cheng S, Lu P, Setty M, Perez AR, Guo A, et al. Ibrutinib resistance in chronic lymphocytic leukemia. N Engl J Med. 2014, 370, 2352-2354.

108. Byrd JC, Harrington BH, O'Brien S, Jones JA, Schuh AS, Devereux S, Chaves J, Wierda WG, Awan FT, Brown JR, Hillmen P, Stephens DM, Ghia P, Barrientos JC, Pagel JM, Woyach J, Johnson D, Huang J, Wang XL, Kaptein A, Lannutti BJ, Covey T, Fardis M, McGreivy J, Hamdy A, Rothbaum W, Izumi R, Diacovo TG, Johnson AJ, Furman RR. Acalabrutinib (ACP-196) in relapsed chronic lymphocytic leukemia. N. Engl. J. Med. 2016, 374, 323-332.

109. Sawalha Y, Bond DA, Alinari L. Evaluating the therapeutic potential of Zanubrutinib in the treatment of relapsed/refractory mantle cell lymphoma: evidence to date. OncoTargets and Therapy. 2020, 13, 6573–6581.

110. Lynch Jr. TJ, Kim ES, Eaby B, Garey J, West DP, Lacouture ME. Epidermal growth factor receptor inhibitor-associated cutaneous toxicities: an evolving paradigm in clinical management. Oncologist. 2007, 12(5), 610-21.

111. Alsadhan A, Cheung J, Gulrajani M, Gaglione EM, Nierma P, Hamdy A, Izumi R, Bibikova E, Patel P, Sun C, Covey T, Herman SEM, Wiestner A. Pharmacodynamic Analysis of BTK Inhibition in Patients with Chronic Lymphocytic Leukemia Treated with Acalabrutinib. Clin. Cancer Res. 2020, 26 (12), 2800-2809.

112. Estupinan TY, Berglof A, Zain R, Smith CIE, Comparative Analysis of BTK Inhibitors and Mechanisms Underlying Adverse Effects. Front. Cell Dev. Biol. 2002, 9, 630942.

113. Dhillon S. Tirabrutinib: first approval, Drugs. 2020, 80(8),835–840.

114. Watterson SH, Liu QJ, Bertrand MB, Batt DG, Li L, Pattoli MA, Skala S, Cheng LH, Obermeier MT, Moore R, Yang Z, Vickery R, Elzinga PA, Discenza L, D'Arienzo C, Gillooly KM, Taylor TL, Pulicicchio C, Zhang YF, Heimrich E, McIntyre KW, Ruan Q, Westhouse RA, Catlett IM, Zheng NY, Chaudhry C, Dai J, Galella MA, Tebben AJ, Pokross M, Li JQ, Zhao RL, Smith D, Rampulla R, Allentoff A, Wallace MA, Mathur A, Salter-Cid L, Macor JE, Carter PH, Fura A, Burke JM, Tino JA. Discovery of Branebrutinib (BMS-986195): a Strategy for Identifying a highly potent and selective covalent inhibitor providing rapid *in vivo* inactivation of Bruton's tyrosine kinase (BTK). J. Med. Chem. 2019, 62, 3228-3250.

115. D. Isenberg, R. Furie, N.S. Jones, P. Guibord, J. Galanter, C. Lee, A. McGregor, B. Toth, J. Rae, O. Hwang, R. Desai, A. Lokku, N. Ramamoorthi, J.A. Hackney, P. Miranda, V.A. de Souza, J.J. Jaller-Raad, A. Maura Fernandes, R. Garcia Salinas, Chinn

LW, Townsend MJ, Morimoto AM, Tuckwell K. Efficacy, safety, and pharmacodynamic effects of the Bruton's tyrosine kinase inhibitor Fenebrutinib (GDC-0853) in systemic lupus erythematosus: results of a phase II, randomized, double-blind, placebo-controlled trial. Arthritis Rheumatol. 2021, 73(10), 1835–1846.

116. Singh J, Petter RC, Baillie TA, Whitty A. The Resurgence of Covalent Drugs. Nat. Rev. Drug Discov. 2011, 10, 307–317.

117. Kalgutkar AS, Dalvie DK. Drug discovery for a new generation of covalent drugs. Expert Opin. Drug Discov. 2015, 7, 561–581.

118. Liu Q, Sabnis Y, Zhao Z, Zhang T, Buhrlage SJ, Jones LH, Gray NS. Developing irreversible inhibitors of the protein kinase cysteinome. Chem. Biol. 2013, 20, 146–159.

119. Bender AT, Gardberg A, Pereira A, Johnson T, Wu Y, Grenningloh R, Head J, Morandi F, Haselmayer P, Liu-Bujalski L. Elucidation of BTK Inhibitor's Selectivity for Different Pathways. Molecular Pharmacology. 2017, 91(3), 208-219.

120. Zhu K, Borrelli KW, Greenwood JR, Day T, Abel R, Farid RS, Harder E. Docking covalent inhibitors: a parameter free approach to pose prediction and scoring, J. Chem. Inf. Model. 2014, 54(7). 1932–1940.

121. Schrödinger Release, 2019-1: LigPrep, Schrödinger, LLC, New York, NY, 2019.

122. Wang J, Guo J, Zhan J, Bu H, Lin J. An in-vitro cocktail assay for assessing compound-mediated inhibition of six major cytochrome P450 enzymes. 2014, 4(4), 270-278.

123. Danker T, Moller C. Early identification of hERG liability in drug discovery programs by automated patch clamp. 2014, 5, 203.

124. Artursson P, Palm K, Luthman K. Caco-2 monolayers in experimental and theoretical predictions of drug transport. Adv Drug Deliv Rev. 2001, 46(1-3), 27-43.

125. Li P, Wang B, Zhang X, Batt SM, Besra GS, Zhang T, et al. Identification of novel benzothiopyranone compounds against Mycobacterium tuberculosis through scaffold morphing from benzothiazinones. Eur J Med Chem. 2018; 160:157-170.

126. Scales HE, Ierna M, Smith KM, et al. Assessment of murine collagen- induced arthritis by longitudinal non-invasive duplexed molecular optical imaging. Rheumatology. 2016, 55, 564-572.

127. Promega Corporation, https://www.promega.com/-/media/files/resources/protocols/kinase-enzyme-appnotes/btk-kinase-assay-protocol.pdf.

128. Yahiaoui A, Meadows SA, Sorensen RA, Cui ZH, Keegan KS, Brockett R, Chen G, Quéva C, Li L, Tannheimer SL. PI3Kδ inhibitor idelalisib in combination with BTK inhibitor ONO/GS-4059 in diffuse large B cell lymphoma with acquired resistance to PI3Kδ and BTK inhibitors. PLoS One. 2017, 12(2), e0171221.

129. Luo FR, Yang Z, Camuso A, Smykla R, McGlinchey K, Fager K, et al. Dasatinib (BMS-354825) Pharmacokinetics and pharmacodynamic biomarkers in animal models predict optimal clinical exposure. Clin Cancer Res. 2006, 12(23), 7180-7186.

130. Gaudio E, Tarantelli C, Kwee I, Barassi C, Bernasconi E, Rinaldi A, Ponzoni M, Cascione L, Targa A, Stathis A, Goodstal S, Zucca E, Berton F. Combination of the MEK inhibitor pimasertib with BTK or PI3K-delta inhibitors is active in preclinical models of aggressive lymphomas. Annals of Oncology. 2016, 27, 1123–1128.

131. Asquith DL, Miller AM, McInnes IB, Liew FY. Animal models of rheumatoid arthritis. Eur. J. Immunol. 2009, 39, 2040-2044.

132. Buscher B, Laakso S, Mascher H, Pusecker K, Doig M, Dillen L, Wagner-Redeker W, Pfeifer T, Delrat P, Timmerman P. Bioanalysis for plasma protein binding studies in

drug discovery and drug development: views and recommendations of the European Bioanalysis Forum. Bioanalysis. 2014, 6(5), 673-682. 130.

133. Raj J, Mohineesh, Ray R, Dogra TD, Raina A. Acute oral toxicity and histopathological study of combination of endosulfan and cypermethrin in wistar rats. Toxicol Int. 2013, 20(1), 61-7.